Modeling of enzymatic reactions: Computational biocatalysis

Walter Thiel

Max-Planck-Institut für Kohlenforschung, Mülheim

- **Overview**
- **QM/MM methodology**
- **Cytochrome P450**
- **Lipases**

BASF – Heraeus, Workshop: Biocatalysis, 24 April 2014

QM/MM approach: General overview

QM: ab initio, DFT, semiempirical

MM: standard force field

QM – MM interactions:

„*electronic embedding*“

$$\hat{H}^{I,O}_{QM-MM} = -\sum_{i,J}\frac{q_J}{r_{iJ}} + \sum_{i,J}\frac{q_J Z_A}{R_{AJ}} + \sum_{A,J}\left(\frac{A_{AJ}}{R^{12}_{AJ}} - \frac{B_{AJ}}{R^{6}_{AJ}}\right)$$

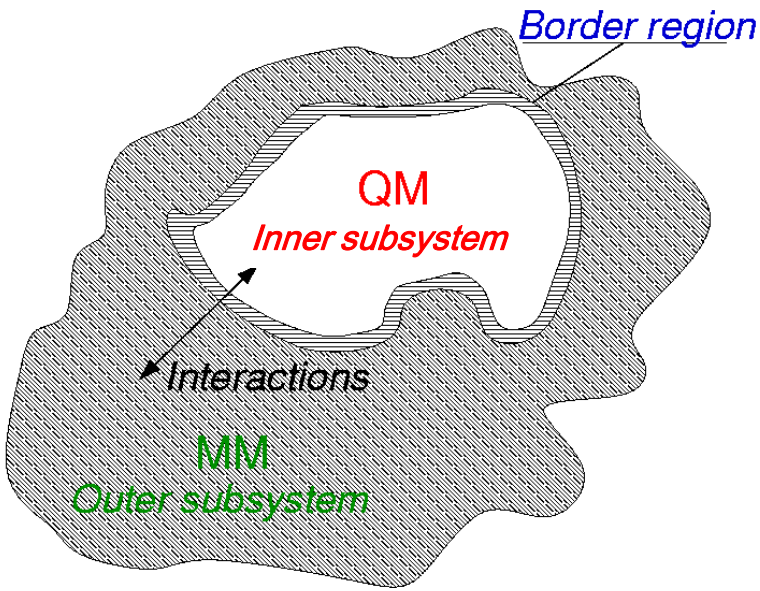

Border region:

- hydrogen link atoms **L**
- charge shift for q(M_1)

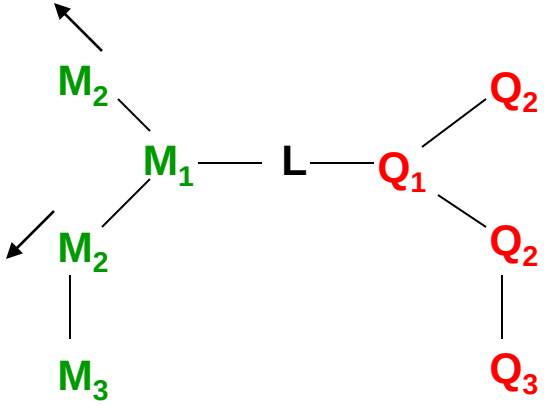

Codes:

ChemShell as control module

Interfaces to standard QM and MM codes

H. M. Senn and W. Thiel, Top. Curr. Chem. **268**, 173-290 (2007).

ChemShell: A modular QM/MM package

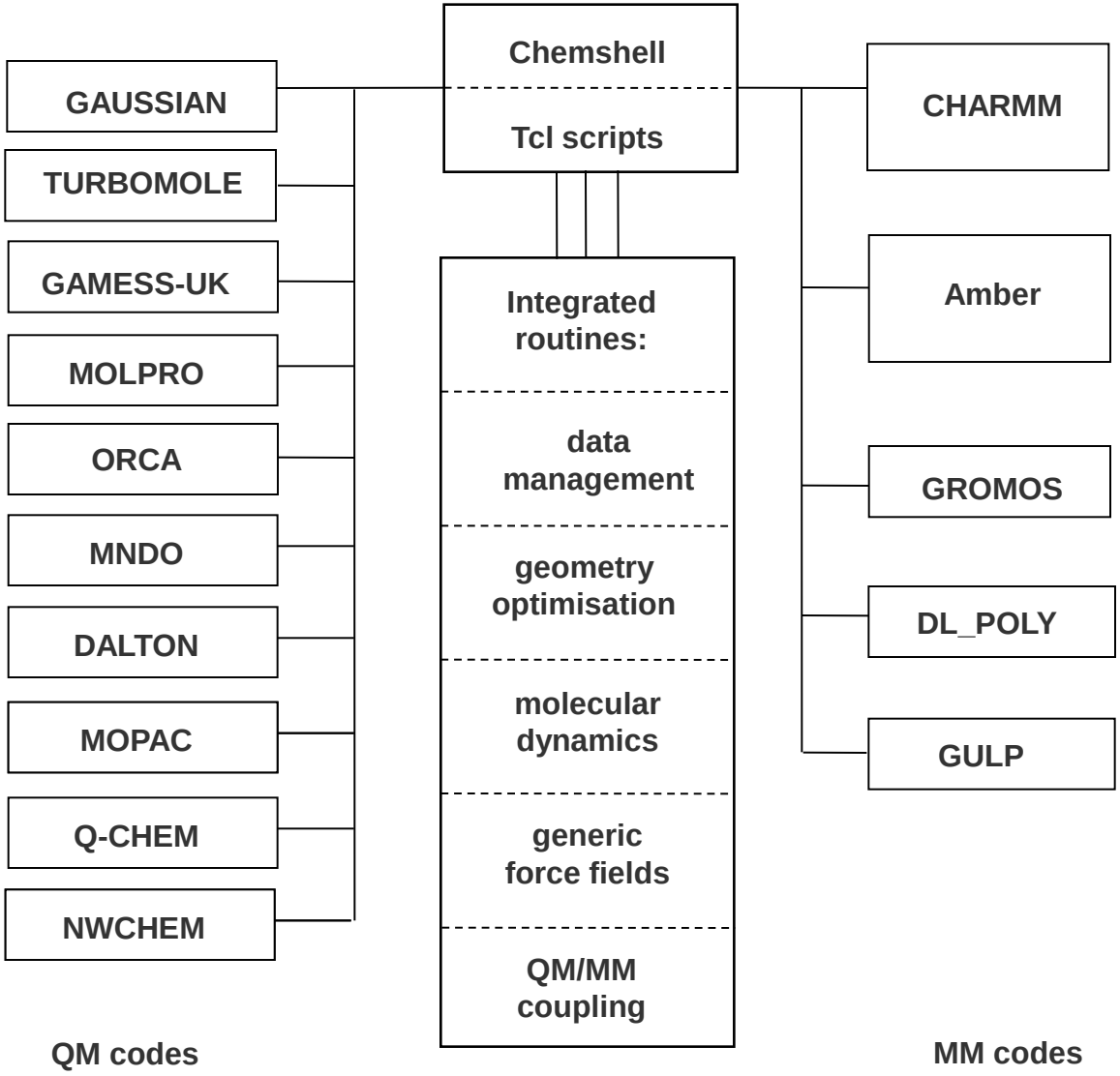

S. Metz et al, WIREs Comput. Mol. Sci. **4**, 101-110 (2014).

http://www.chemshell.org

Consensus QM/MM approach to biomolecular modeling

- Total system size of 10000-40000 atoms including solvent
- Active-site QM region of typically 50-100 atoms
- Standard DFT as QM component (typically B3LYP)
- Standard force field as MM component (CHARMM, GROMOS, AMBER)
- Electrostatic QM/MM embedding
- QM/MM boundary treated by link atom scheme
- Geometry optimization of a limited number of snapshots
- Computation of reaction paths and energy profiles

H. M. Senn and W. Thiel, Angew. Chem. Int. Ed. **48**, 1198-1229 (2009).

Possible improvements of the consensus QM/MM approach

- Larger active-site QM regions
- High-level correlated ab initio methods as QM components
- Dispersion corrections for lower-level QM methods
- Polarized force fields as MM component
- Polarized QM/MM embedding
- More refined QM/MM boundary treatments
- Proper sampling through molecular dynamics or Monte Carlo methods
- Computation of free energy profiles
- Adaptive QM/MM partitioning
- Extension to excited-state QM/MM modeling
- Extension to three-layer QM/MM/continuum approaches
- Periodic boundary conditions versus finite model systems

PHBH : p-hydroxybenzoate hydroxylase

Aromatic hydroxylation of p-hydroxybenzoate

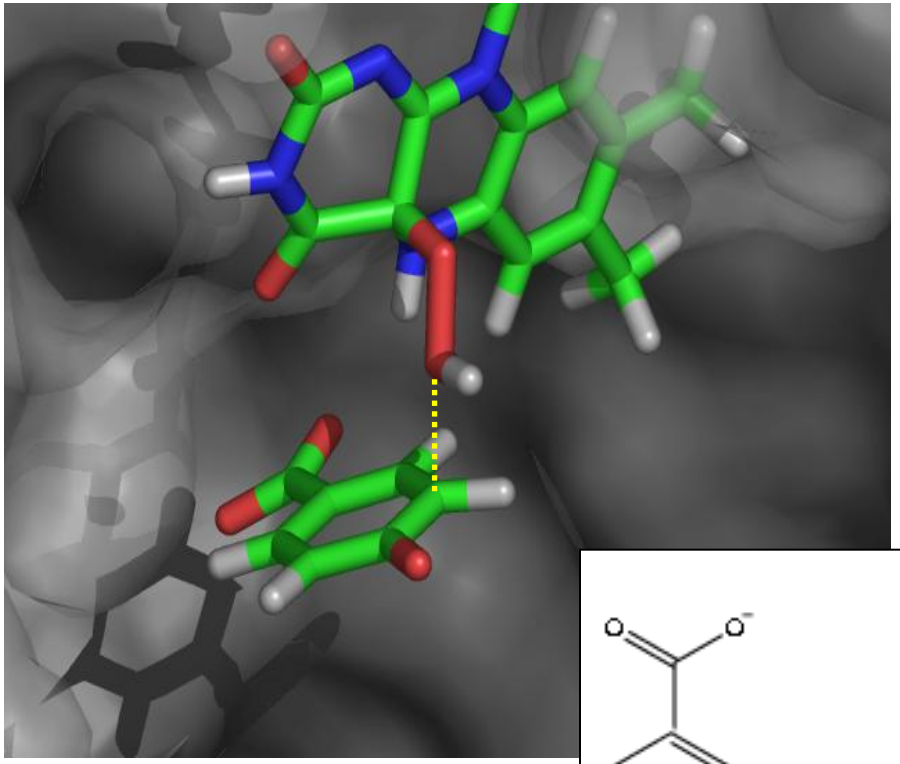

- rate-determining step: oxygen transfer from cofactor FADHOOH to *p*-OHB (FAD: flavin adenine dinucleotide)
- electrophilic aromatic substitution with heterolytic cleavage of the peroxide bond
- activation energy: 12 kcal/mol

Reaction mechanism of key step in PHBH

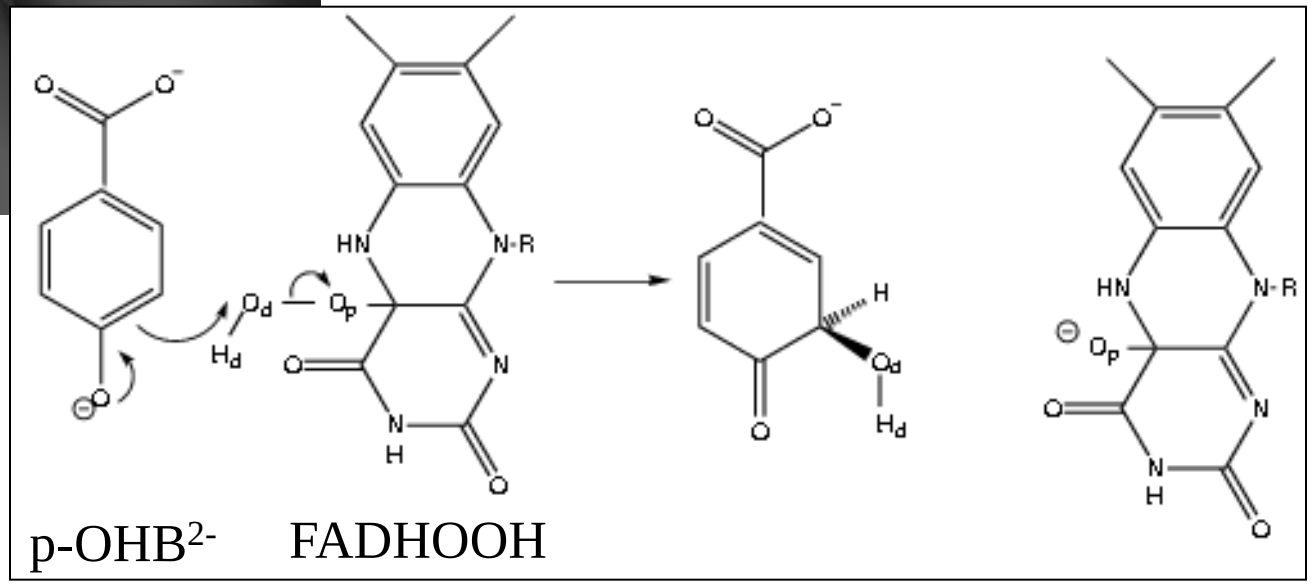

PHBH : General setup

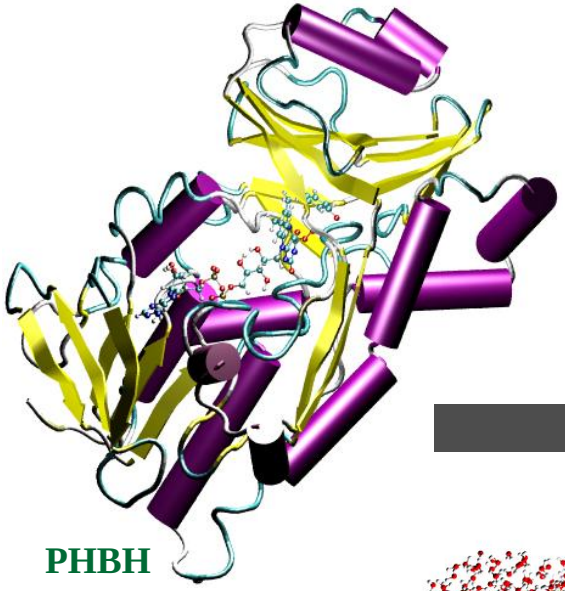

PHBH
7004 atoms

- solvate
- EM – MD cycles
- snapshots from subsequent MD as initial configurations for QM/MM
- substrate, cofactor restrained

solvate

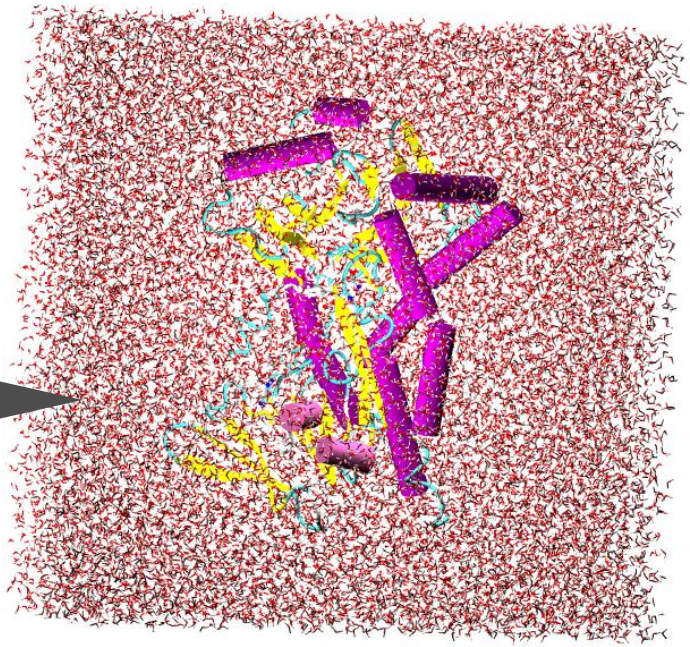

PHBH solvated in cubic box 75000 atoms

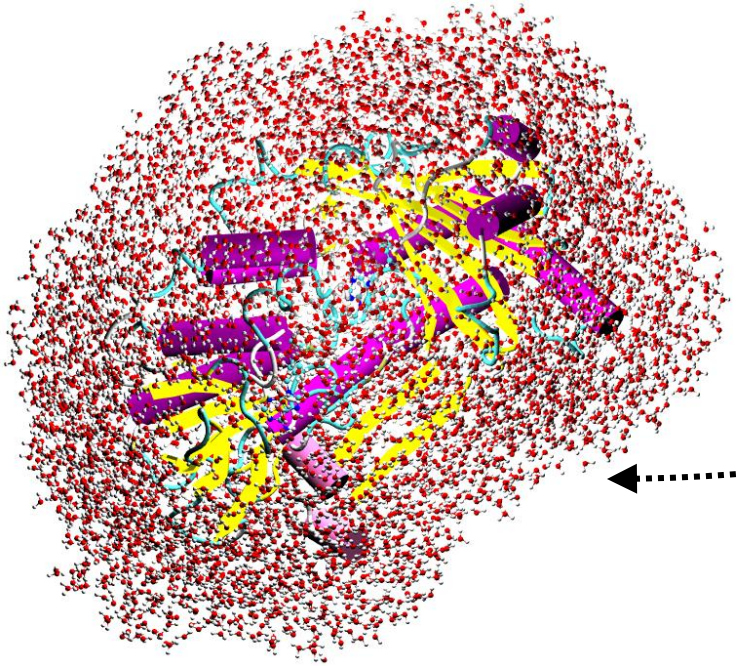

PHBH-water cluster 25000 atoms

- cut out PHBH-water aggregate
- outermost water layer fixed

SP LMP2/GROMOS and LCCSD(T0)/GROMOS barriers (TZ basis)

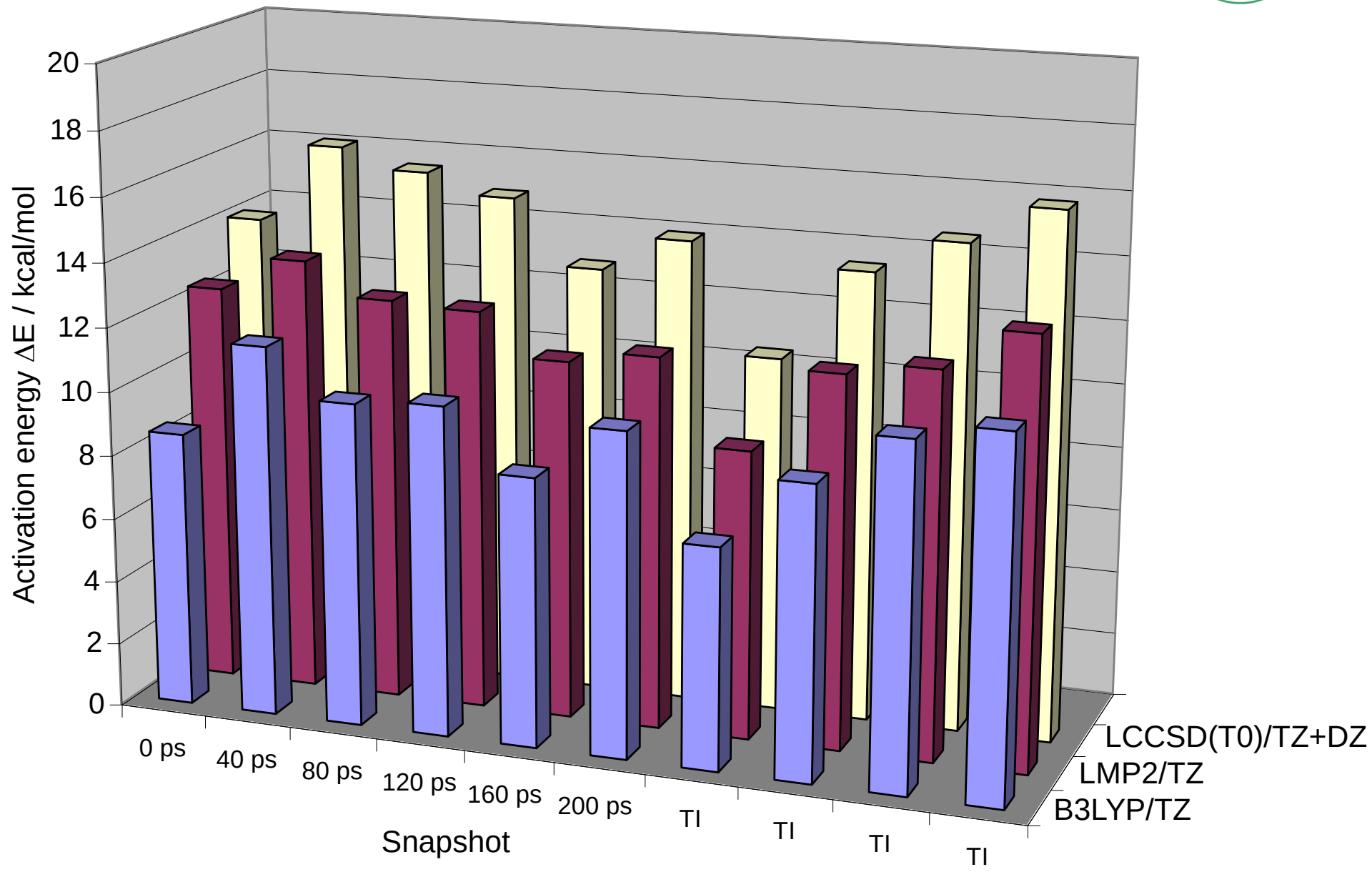

PHBH and CM: Comparison of barriers

PHBH: p-hydroxybenzoate hydroxylase, electrophilic aromatic substitution

CM: chorismate mutase, pericyclic Claisen rearrangement

Computed QM/MM activation enthalpies (kcal/mol)[a]

Method	HF	B3LYP	LMP2	LCCSD	LCCSD(T0)	Experiment
CM	28.3	10.2	9.5	18.7	13.1	12.7
PHBH[b]	36.7	8.4	10.7	20.2	13.3	12.0

(a) Average of 16 (CM) or 10 (PHBH) single-point calculations at B3LYP/MM optimized geometries, zero-point energy and 300 K thermal corrections from QM calculations on cluster models, aug-cc-VTZ basis on oxygen and cc-pVTZ basis on all other atoms, MM=CHARMM for CM and MM=GROMOS for PHBH.

(b) Average AM1/GROMOS values for PHBH: 22.8 kcal/mol

Accurate electronic structure methods and transition state theory describe enzymatic reactions quantitatively.

F. Claeyssens, J. N. Harvey, F. R. Manby, R. A. Mata, A. J. Mulholland, K. E. Ranaghan, M. Schütz, S. Thiel, W. Thiel, and H.-J. Werner, Angew. Chem. **118**, 7010 (2006).

QM/MM free energy calculations

- **Essential for proper treatment of reaction rates**
- **Important for understanding the origin of enzymatic catalysis through comparison of free energy barriers in solution and in the enzyme**
- **Affordable: semiempirical QM/MM**
- **Challenging: ab initio QM/MM**

H. Hu and W. Yang, Annu. Rev. Phys. Chem. **59**, 573-601 (2008).

ChemShell: Simulation techniques

Sampling methods implemented in ChemShell:

-Thermodynamic integration [1]

- Umbrella sampling [2]

- Approximate free-energy perturbation methods [3]

Novel analysis method: **Umbrella integration** [2,4]

Consistent results for free-energy barriers in PHBH [1-4]

from AM1/GROMOS calculations, for example:

24.2 ± 0.5 kcal/mol [1] and 24.3 ± 0.5 kcal/mol. [2,4]

[1] H. M. Senn, S. Thiel and W. Thiel, J. Chem. Theory Comput. **1**, 494 (2005).

[2] J. Kästner and W. Thiel, J. Chem. Phys. **123**, 144104 (2005).

[3] J. Kästner, H. M. Senn, S. Thiel, N. Otte and W. Thiel, J. Chem. Theory Comp. **2**, 452 (2006).

[4] J. Kästner and W. Thiel, J. Chem. Phys. 124, 234106 (2006).

Thermodynamic integration

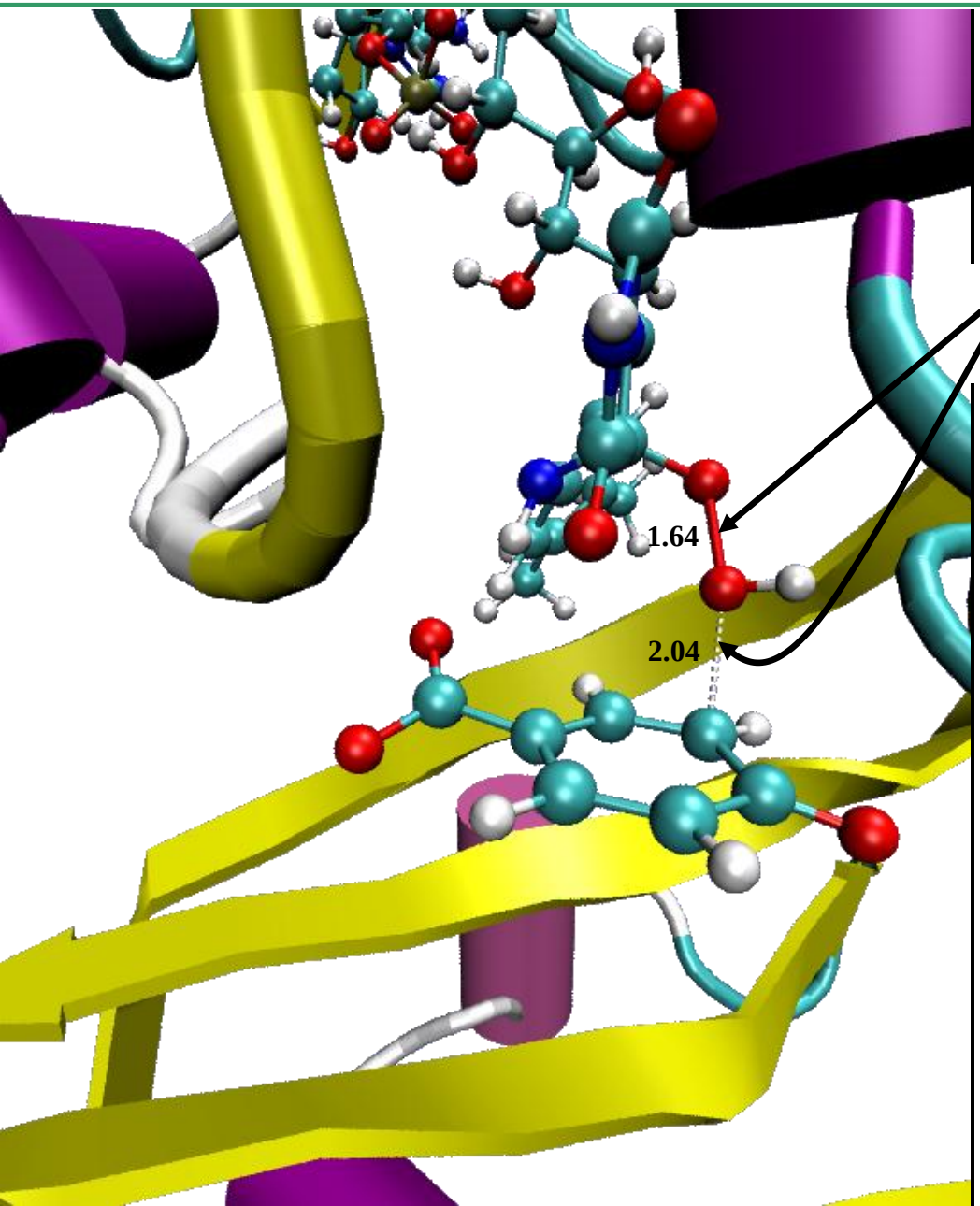

$$\Delta A_{BA} = A(\lambda_B) - A(\lambda_A) = \int_{\lambda_A}^{\lambda_B} \left\langle \frac{\partial H(\lambda)}{\partial \lambda} \right\rangle_{\lambda} d\lambda$$

- constrain difference of distances

$$\lambda = d(\mathrm{O_d} - \mathrm{C_3}) - d(\mathrm{O_p} - \mathrm{O_d})$$

- implemented into SHAKE algorithm of DL_POLY

Start: optimised transition states,
optimised reactant states

- 5 ps QM/MM MD
  Berendsen thermostat (300 K)

- 35 ps QM/MM MD
  Nose Hoover thermostat (300 K)

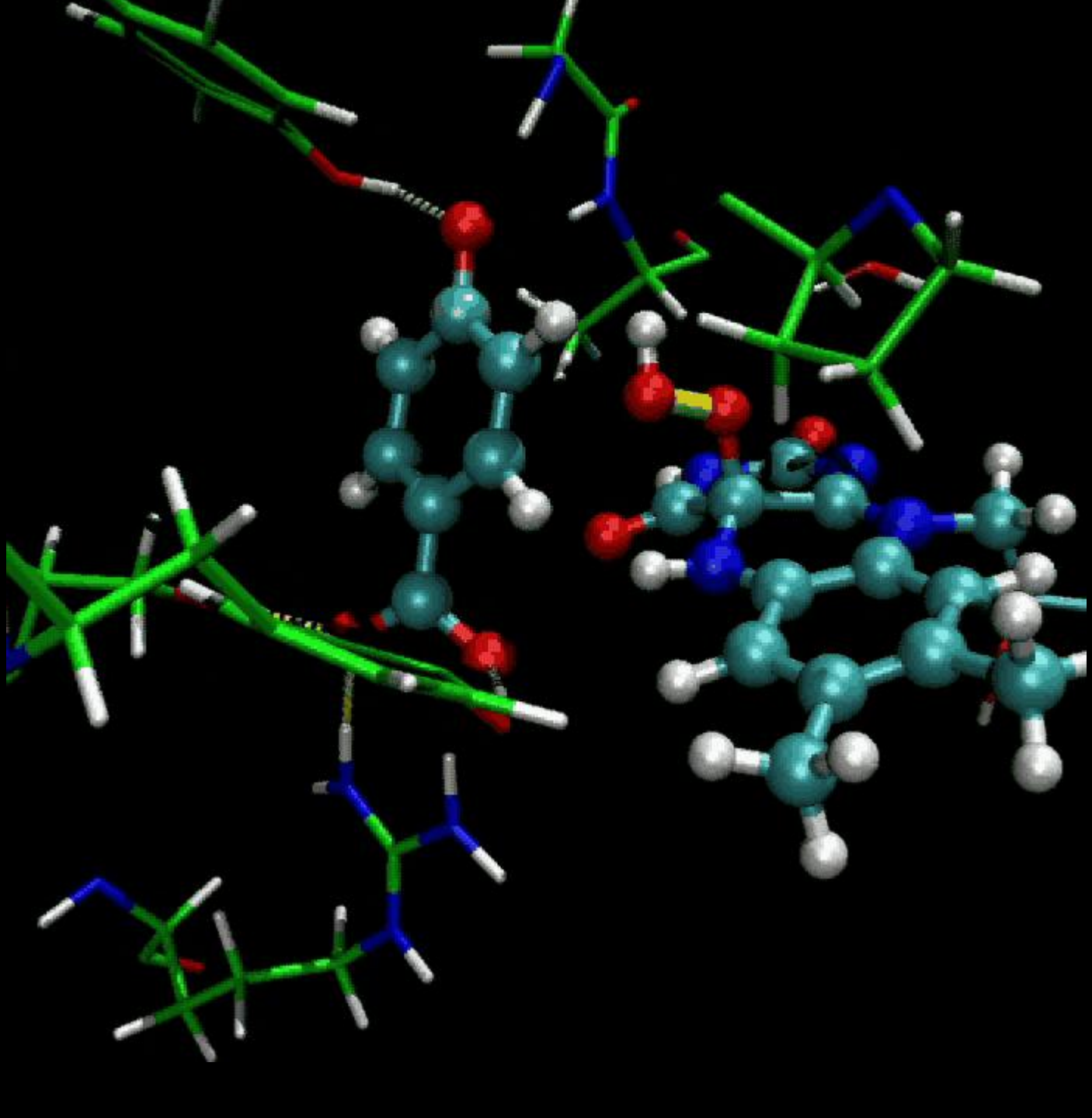

PHBH : Role of Pro293

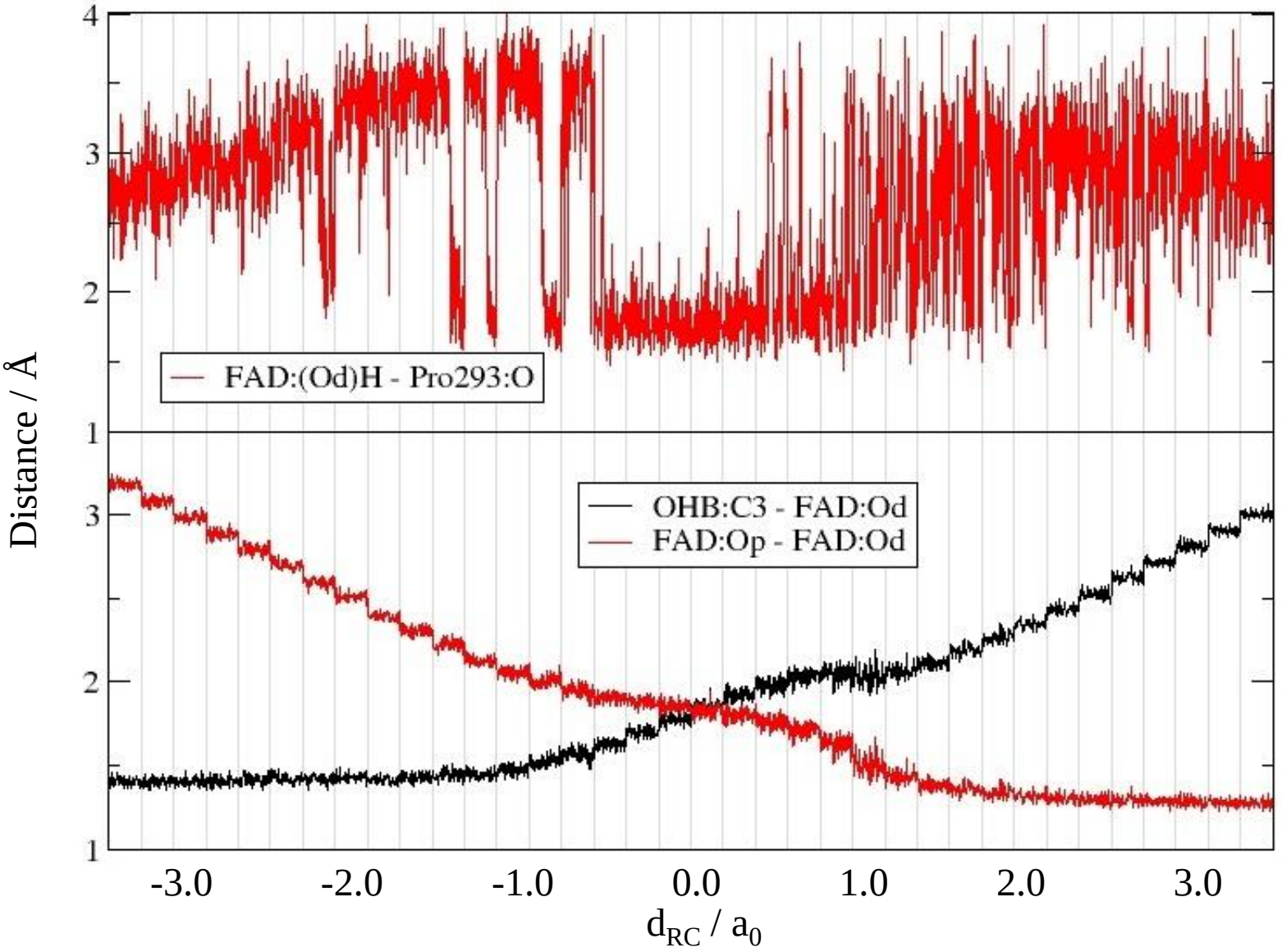

Chorismate mutase: Entropic contribution to barrier

- Experimental data available for *Bacillus subtilis* chorismate mutase [1]
- SCC-DFTB/CHARMM data from 10 forward and backward reaction paths using umbrella sampling and umbrella integration as implemented in ChemShell [2]

	$\Delta H^{\ddagger}$(kcal/mol)	$-T\Delta S^{\ddagger}$(kcalmol)	S(eu)
Experiment	12.7 ± 0.4	2.7 ± 0.4	-9.1 ± 1.2
QM/MM	6.6 ± 1.3	2.2 ± 0.5	-7.2 ± 1.2

- Note: Large spread in experimental entropies [1] for reaction in water, three different enzymes, and two different catalytic antibodies.
- Note: Related QM/MM free energy studies in other groups (e.g., in Bristol and Tsukuba).

[1] P. Kast, M. Asif-Ullah and D. Hilvert, Tetrahedron Lett. **37**, 2691 (1996).

[2] H. M. Senn, J. Kästner, J. Breidung and W. Thiel, Can. J. Chem. **87**, 1322 (2009).

QM/MM free energy barriers in enzymes

Methods applied:

- Semiempirical QM/MM-MD simulations
- DFT/MM free energy perturbation

Enzymatic reactions studied:

- p-Hydroxybenzoate hydroxylase, electrophilic substitution
- Fluorinase, nucleophilic substitution
- Cytochrome P450cam, hydrogen abstraction by Compound I
- Cystein protease, proton transfer involving His199/Cys29

Results:

- Barriers and free energy barriers differ by less than 1 kcal/mol
- Similar reaction profiles

H. M. Senn, J. Kästner, J. Breidung and W. Thiel, Can. J. Chem. **87**, 1322 (2009).

QM/MM studies on ground-state enzyme reactivity

Cytochrome P450	[24]
p-Hydroxybenzoate hydroxylase	[9]
Cysteine proteases	[4]
Acetylene hydratase	[3]
Aldehyde oxidoreductase	[3]
Chorismate mutase	[3]
Lipases	[3]
Xanthine oxidase	[3]
Cyclohexanone monooxygenase	[2]
Fluorinase	[2]
4-Oxalocrotonate tautomerase	[2]
Vanadium haloperoxidases	[2]
Lysine-specific demethylase 1	[1]
LOV photoreceptor protein YtvA	[1]
Fosfomycin resistance protein	[1]
Aldoxime dehydratase	[1]
Retaining glycosyltransferase LgtC	[1]
Cysteine dioxygenase	[1]
Dihydrofolate reductase	[1]
Triosephosphate isomerase	[1]

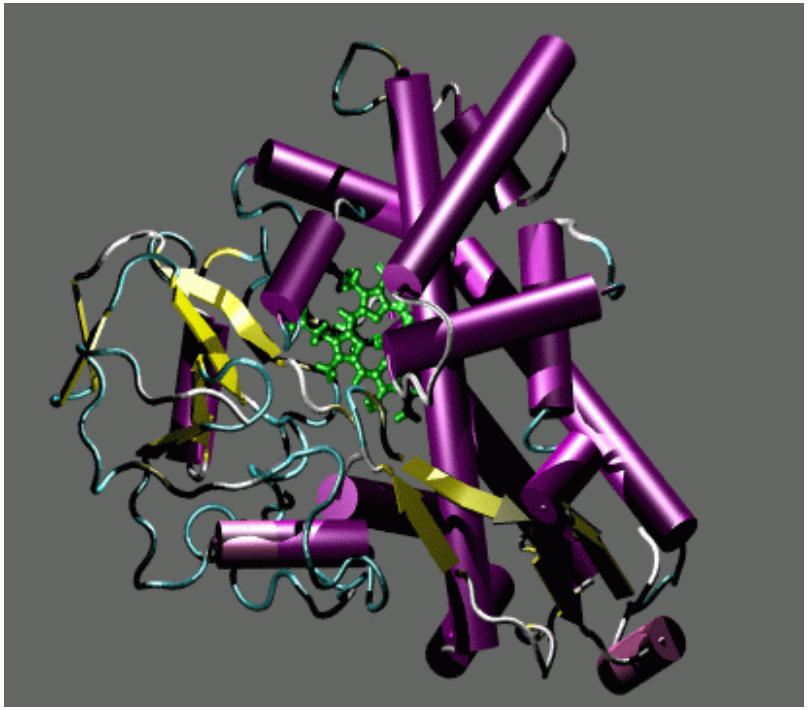

[Number of publications from our group]

Cytochrome $P450_{Cam}$ (Pseudomonas Putida)

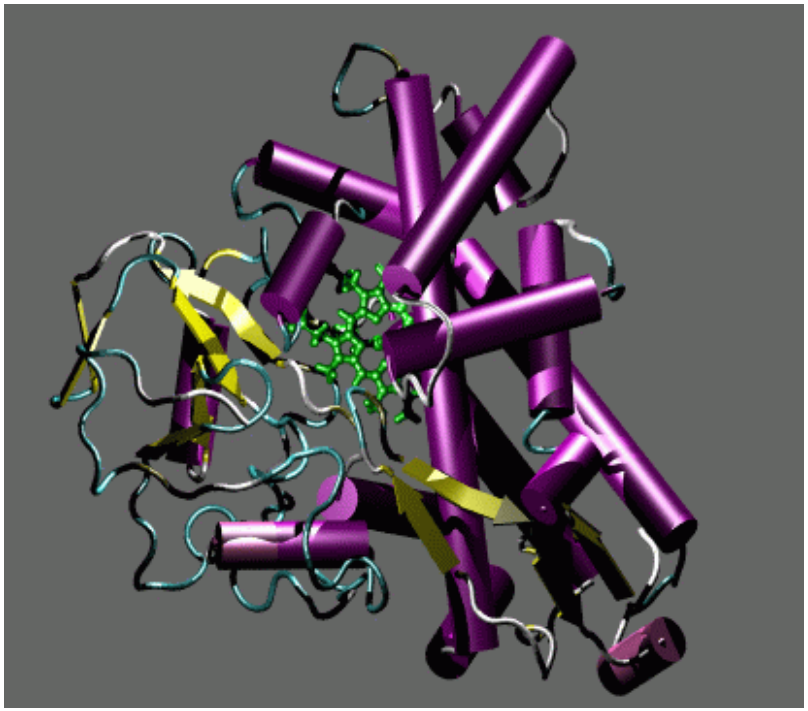

- heme protein, thiolato ligand
- completely buried active site
- soluble - extensively characterized by biochemical / biophysical techniques
- X-ray structures for various intermediates of the catalytic cycle
- natural substrate camphor, also other compounds
- biohydroxylation of non-activated C-H bonds

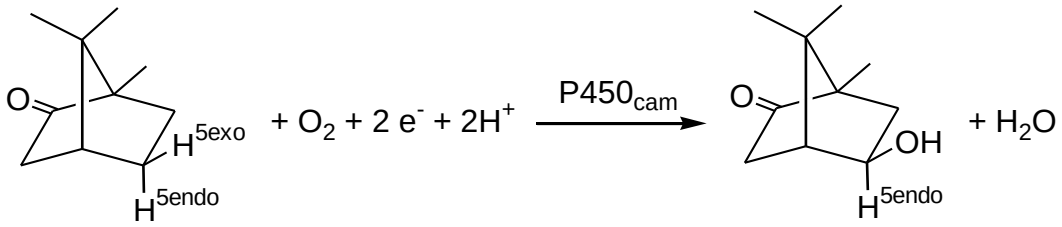

camphor

CYP450: Catalytic cycle

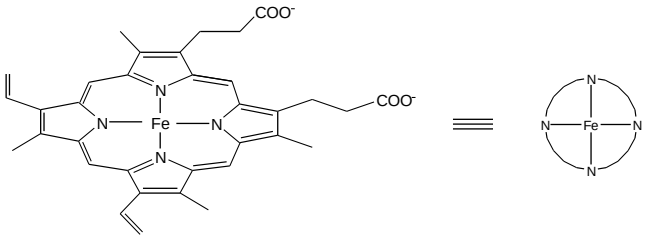

Mechanistic features:

- **electrons from NADPH (2 → 3, 4 → 5)**
- **binding of molecular oxygen (3 → 4)**
- **active species 6 (Compound I) not observed experimentally**
- **hydroxylation mechanism 6 → 8 under dispute (rebound mechanism assumed)**

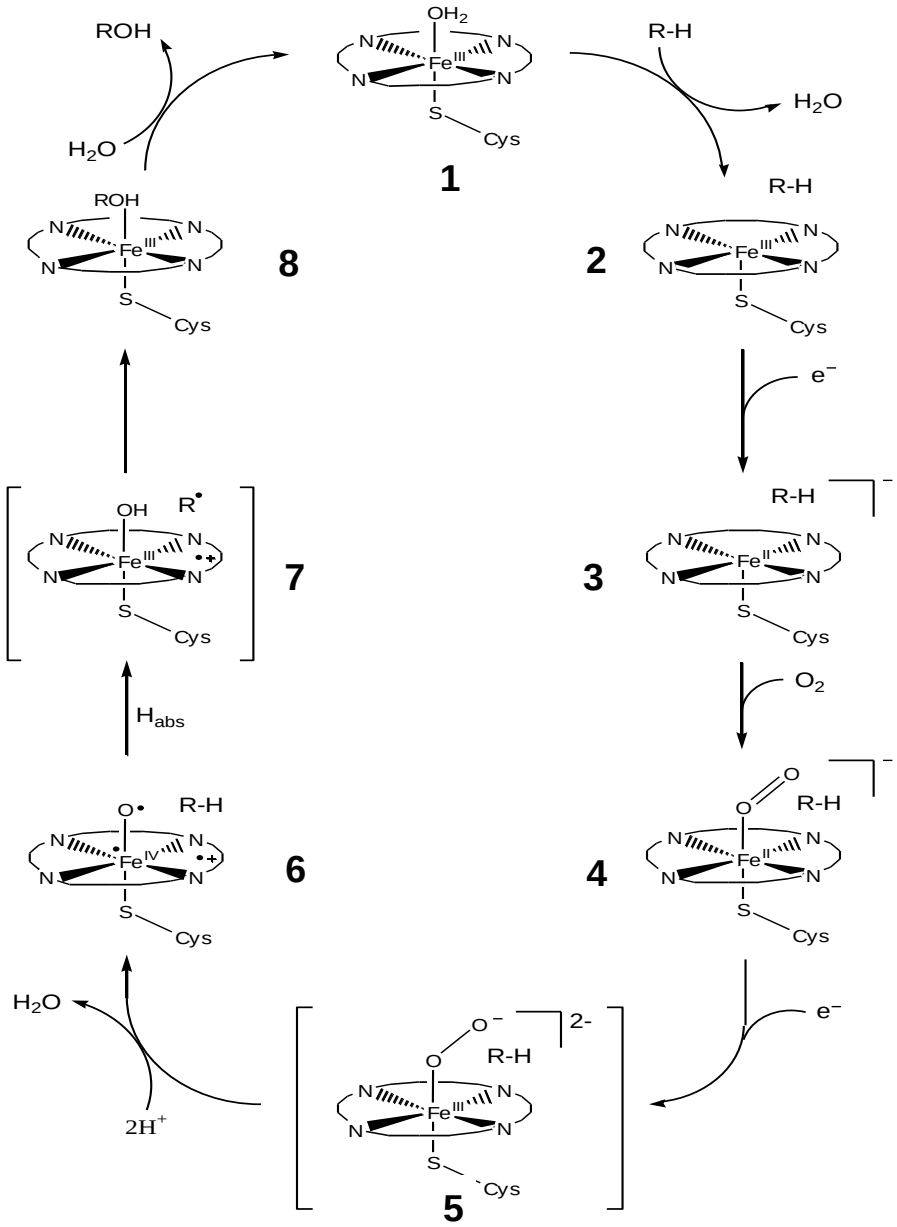

Theoretical approaches to Compound I

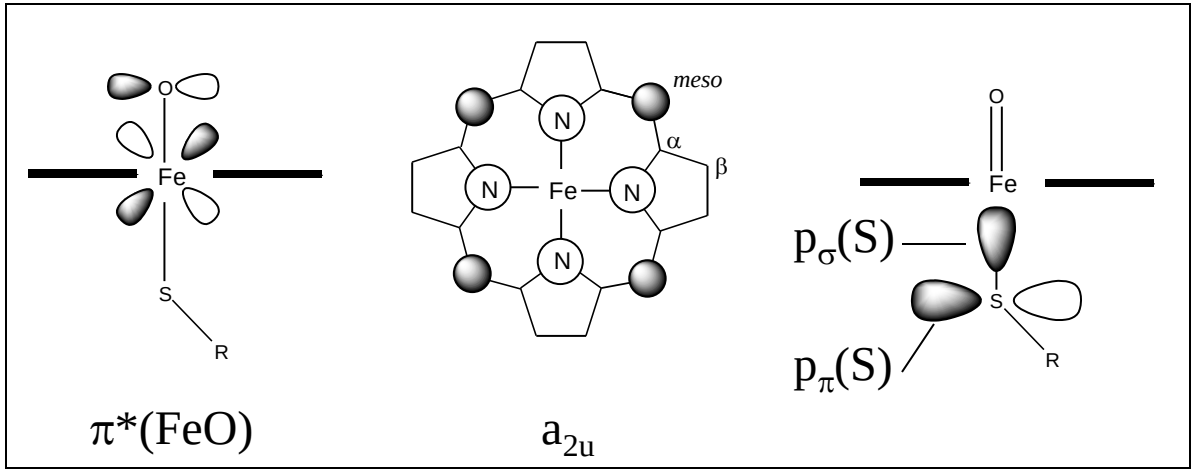

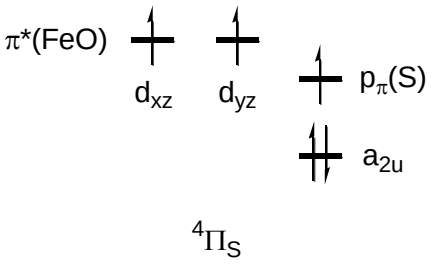

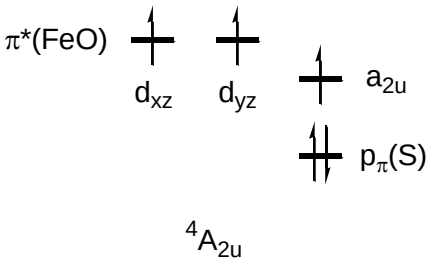

Gas phase model calculations

- **[FeO(porph)(SMe)]**
  Antony et al. 1997;
  Green 1999:
  Π_S **character**
- **[FeO(porph)(SH)]**
  Harris & Loew 1998;
  Filatov et al. 1999:
  A_{2u} **character**

- Doublet and quartet states close in energy ($^{2,4}A_{2u}$ normally below $^{2,4}\Pi_S$)
- Electronic nature sensitive to substituent at sulfur (Ogliaro, Shaik *et al.* 2000)

QM/MM vs. isolated state (gas phase): Unpaired spin densities

R1:
SH

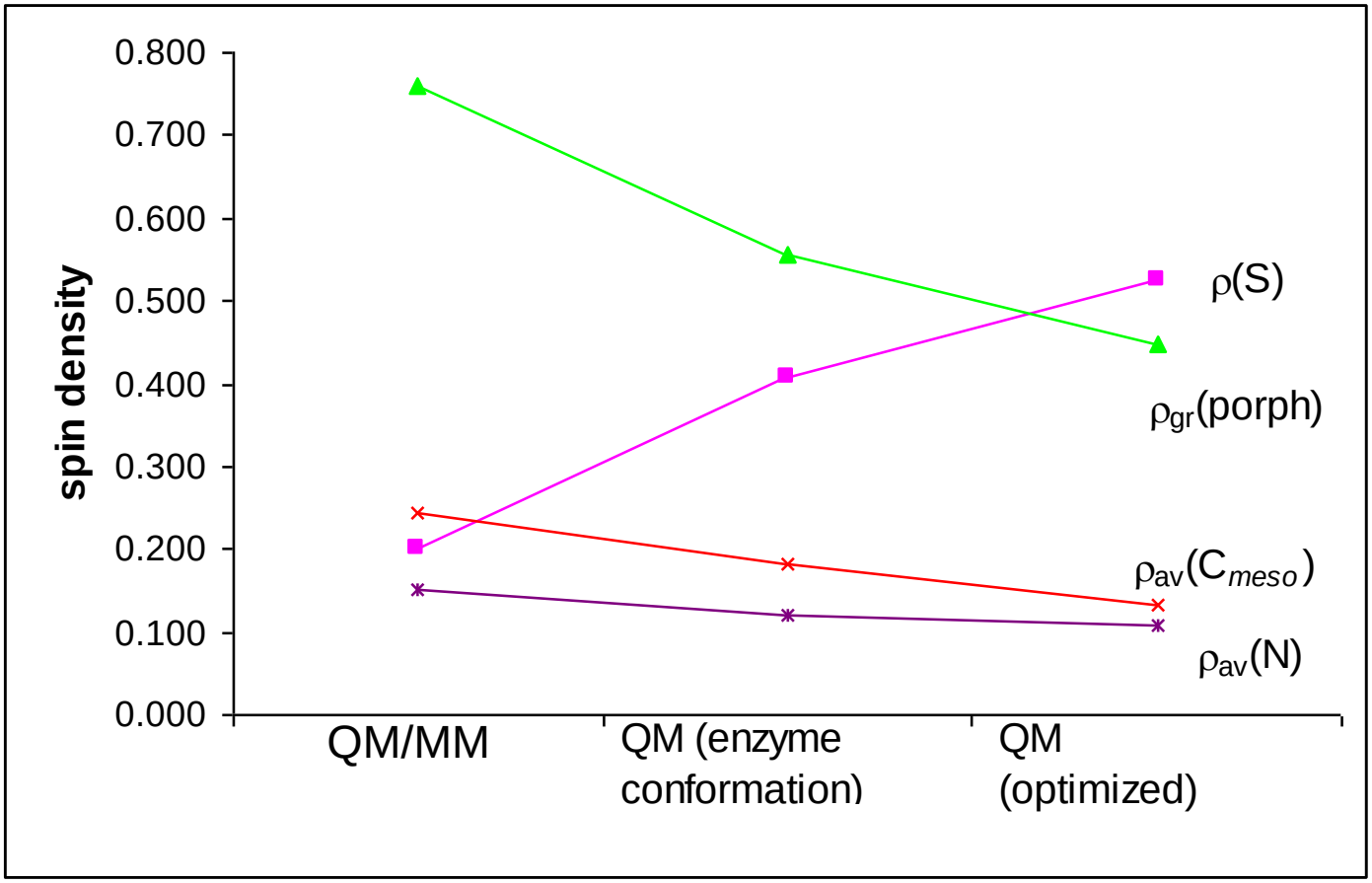

B3LYP,

basis B3

J. C. Schöneboom, H. Lin, N. Reuter, W. Thiel, S. Cohen, F. Ogliaro, S. Shaik, J. Am. Chem. Soc. **124**, 8142 (2002).

H-bond interactions within the Cys357 loop

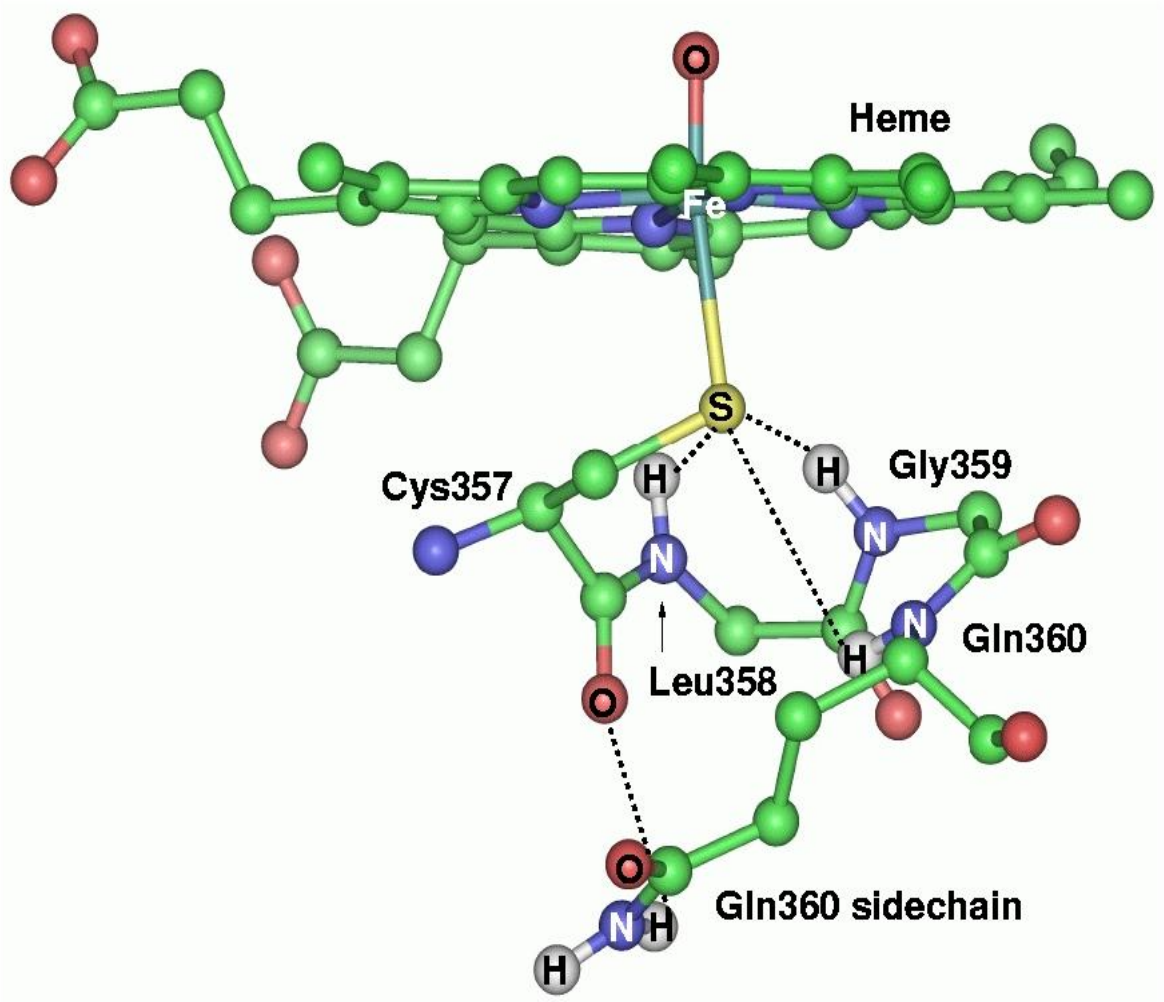

Chloroperoxidase Compound I (CPO-I)

- Chloroperoxidase is the only thiolate-ligated heme enzyme whose Compound I has been characterized spectroscopically.

- The spin density distribution in CPO-I has recently been determined in a rapid freeze-quench ENDOR study:

  The radical is predominantly on the porphyrin, with $\rho_s \leq \rho_{max} \approx 0.23$.

  As the active site of CPO is essentially identical with that of cytochromes P450, we further suggest that the same … applies to P450-I.

- Experimental results confirm B3LYP/CHARMM predictions.

S. H. Kim, R. Perera, L. P. Hager, J. H. Dawson and B. M. Hoffman, JACS 1**28**, 5598 (2006).

Proposed mechanisms for C–H hydroxylation by Compound I

Contradictory experimental findings:

- Product analysis, KIE- measurements:

⇒ rebound mechanism

- Radical clock experiments [1]: apparent lifetimes of possible intermediates too short (τ = 80 – 200 fs)

⇒ competing reaction channels, e.g. oxene insertion [2] **?**

⇒ high-spin and low-spin states involved (two-state-reactivity) [3] **?**

⇒ influence of protein pocket **?**

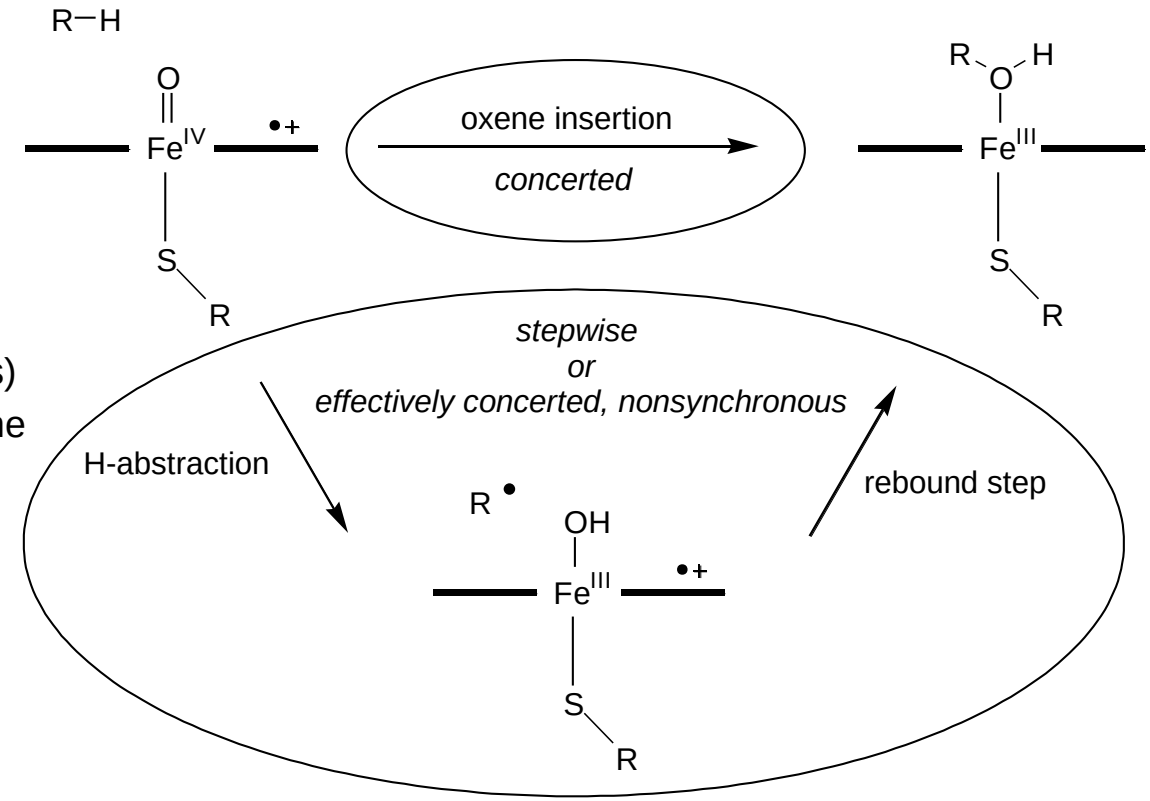

[1] M. Newcomb and P. H. Toy, Acc. Chem. Res. **33**, 449 (2000).
[2] M. Newcomb, M.-H. Le Tadi-Biadatti, D. L. Chestney, E. S. Roberts, and P. F. Hollenberg, JACS **117**, 12085 (1995).
[3] S. Shaik, M. Filatov, D. Schröder, and H. Schwarz, Chem. Eur. J. **4**, 193 (1998).

Mechanism of C–H hydroxylation: Energy profile

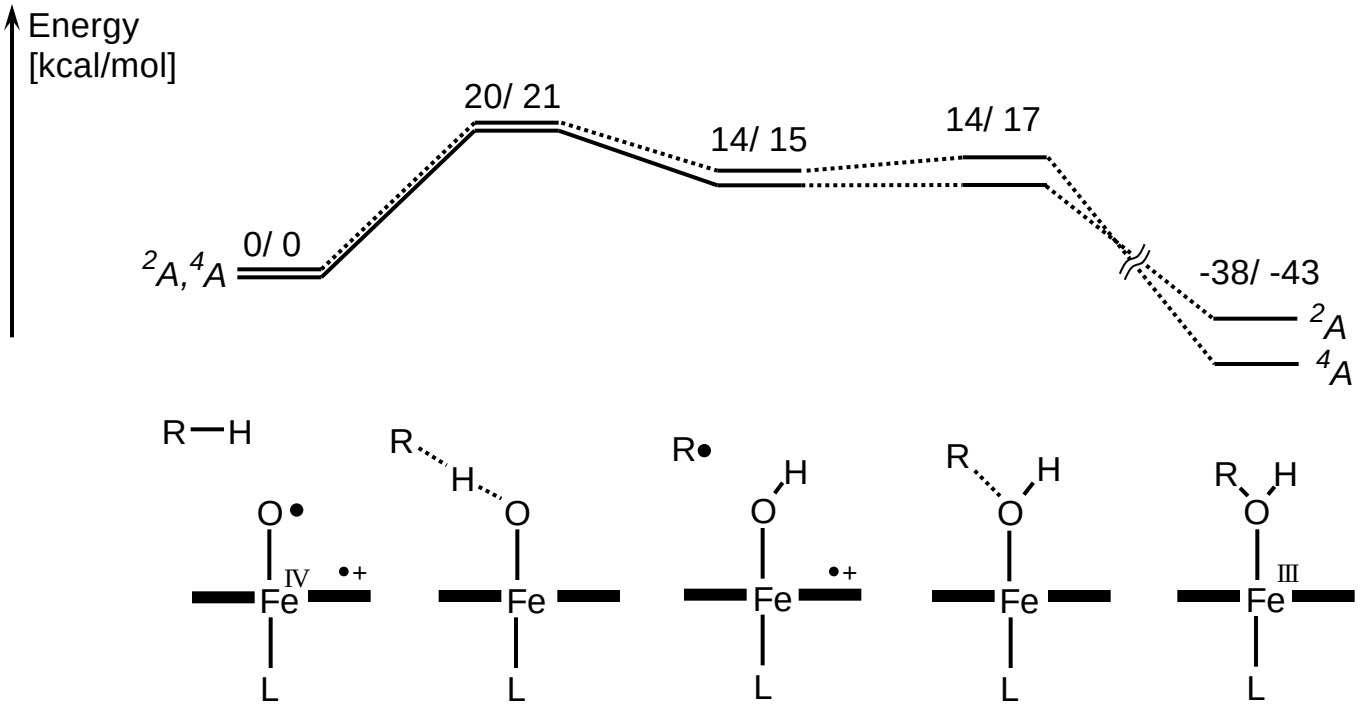

QM/MM geometry optimizations, R1pro/B1
Two-state reactivity confirmed

J. C. Schöneboom, S. Cohen, H. Lin, S. Shaik, and W. Thiel, J. Am. Chem. Soc. **126**, 4017-4034 (2004).

Rebound barriers for quartet / doublet: MO diagram

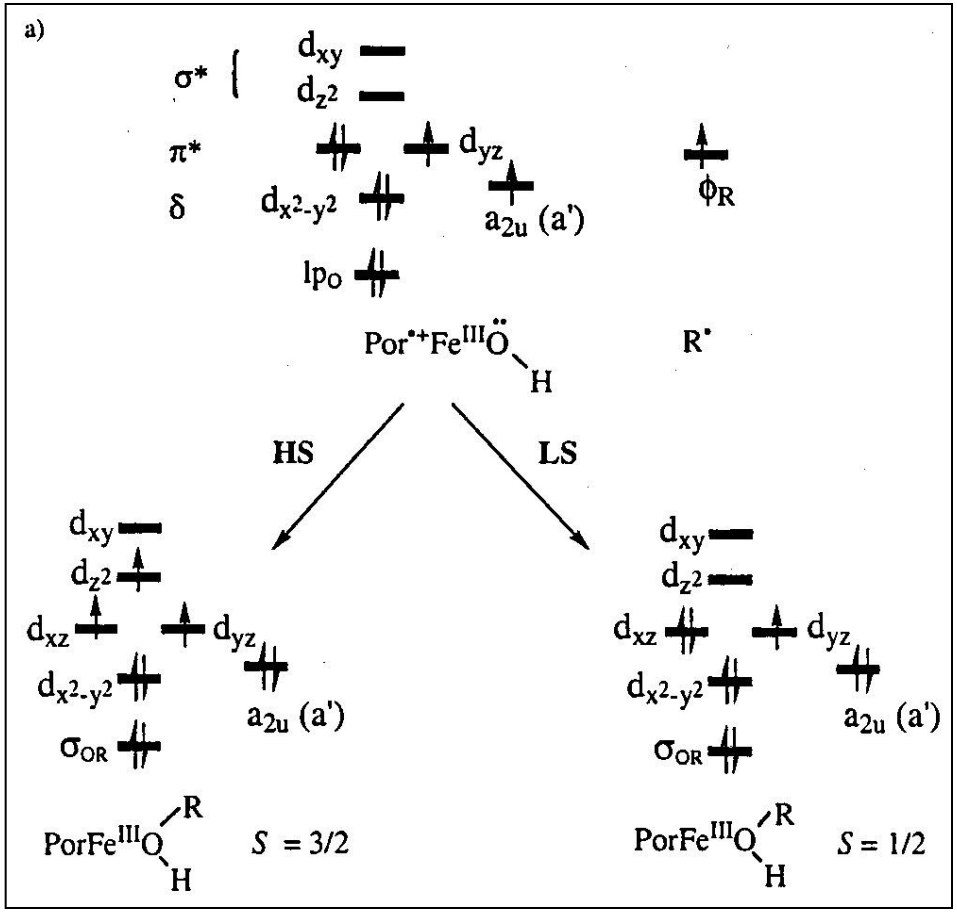

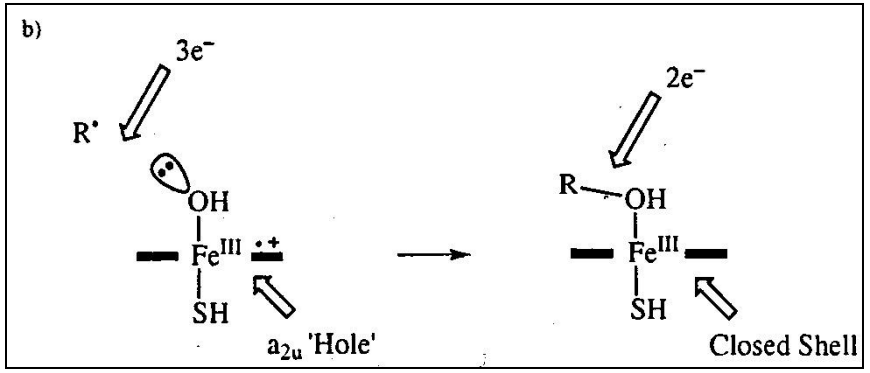

Electronic situation during rebound step:

a) MO diagram

→ rebound barrier in HS state due to occupation of antibonding orbital

b) electron counting diagram

→ filling of „porphyrin hole“

N. Harris, S. Cohen, M. Filatov, F. Ogliaro and S. Shaik, Angew. Chem. Int. Ed. **39**, 2003 (2000).

Catalytic role of water903

- Water903 acts as a **catalyst** for hydrogen abstraction. The stabilization of the transition state arises from favorable electrostatic interactions in **hydrogen bonds** that are stronger in the transition state due to an increasing negative charge at the oxo atom. The computed barrier is lowered by 4 kcal/mol.

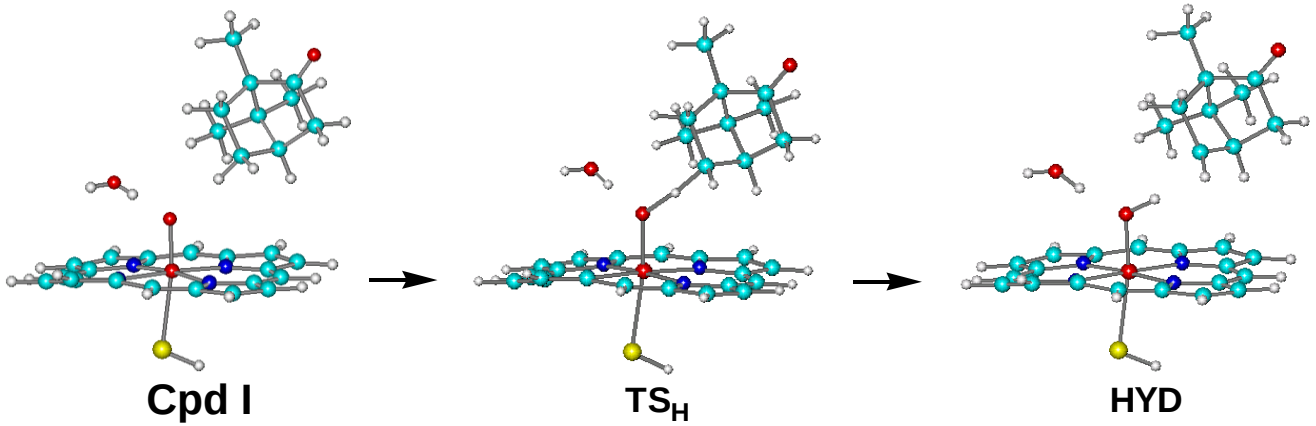

- One water molecule is liberated during the conversion of Cpd 0 to Cpd I :

$$Por(SR)FeOOH^- + H^+ \longrightarrow Por(SR)Fe{=}O + H_2O$$

A. Altun, V. Guallar, R. A. Friesner, S. Shaik, and W. Thiel, J. Am. Chem. Soc. **128**, 3924-3925 (2006).

Conversion of Cpd 0 to Cpd I

Mechanism I

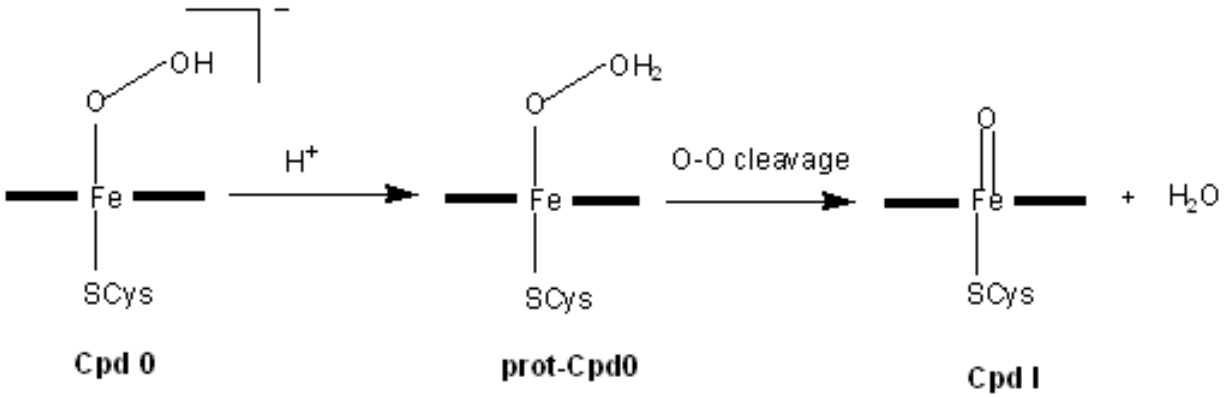

Cpd 0 prot-Cpd0 Cpd I

Mechanism II

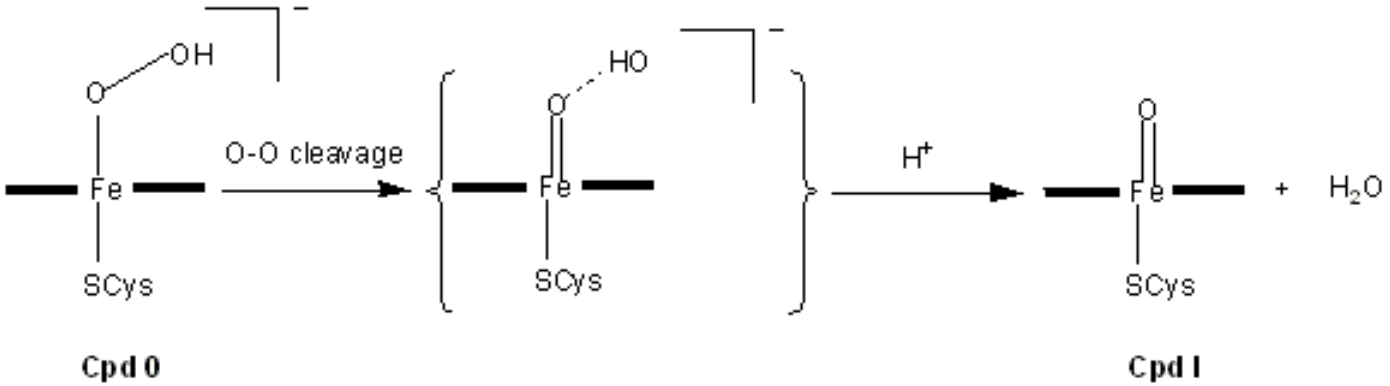

Cpd 0 Cpd I

Glu366 channel: protonated Glu366 as proton source
Asp251 channel: protonated Asp251 as proton source

D. Kumar, S. P. de Visser, W. Thiel, S. Shaik et al., J. Phys. Chem. B **109**, 19946-19951 (2005).
J. Zheng, D. Wang, W. Thiel, and S. Shaik, J. Am Chem. Soc. **128**, 13204-13215 (2006).

Asp-II mechanism: B3LYP/CHARMM study

Protein solvated by water, 24988 atoms, 62-atom QM region (DQ1) containing Por(SH)FeOOH, Asp251 (CH_3COOH), Thr252 (C_2H_5OH), and water901, extended 79-atom QM region (DQ3) also containing Arg186 ($C_2H_5NHC(NH2)_2$); UB3LYP/B1 data.

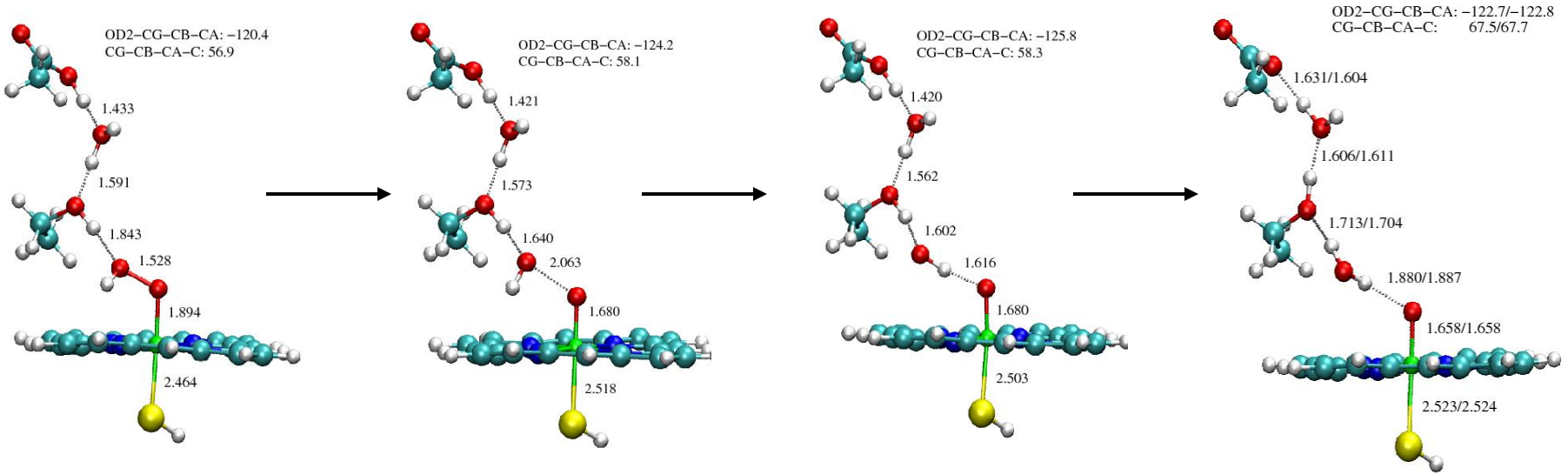

ΔE (kcal/mol)	**0.0**	**14.4**	**11.7**	**(14.2)**	**-0.2**
	Cpd 0	**TS1**	**IC1**	**(scan)**	**Cpd I**

Coupling and uncoupling reaction

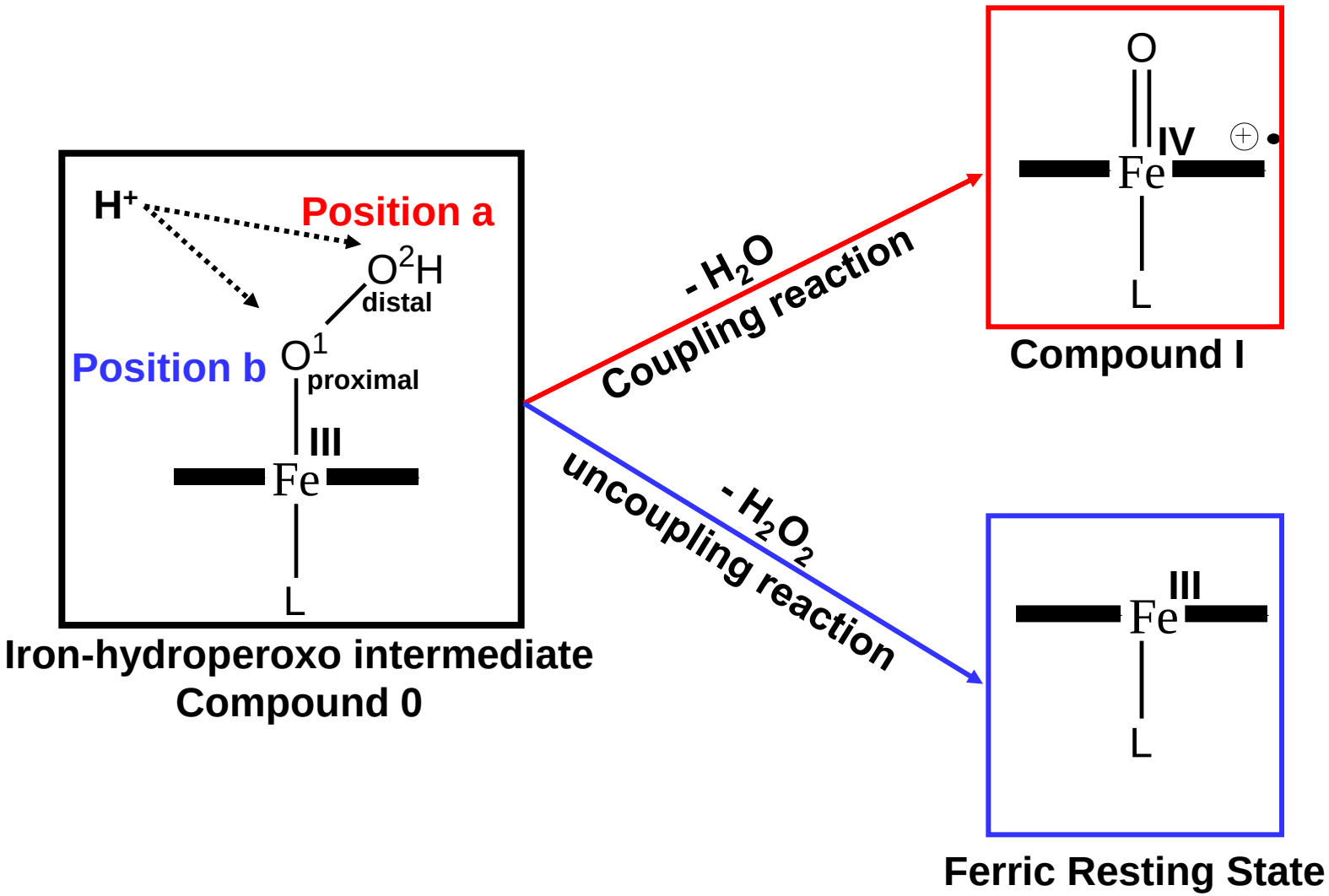

Coupling and uncoupling reactions - WT enzyme

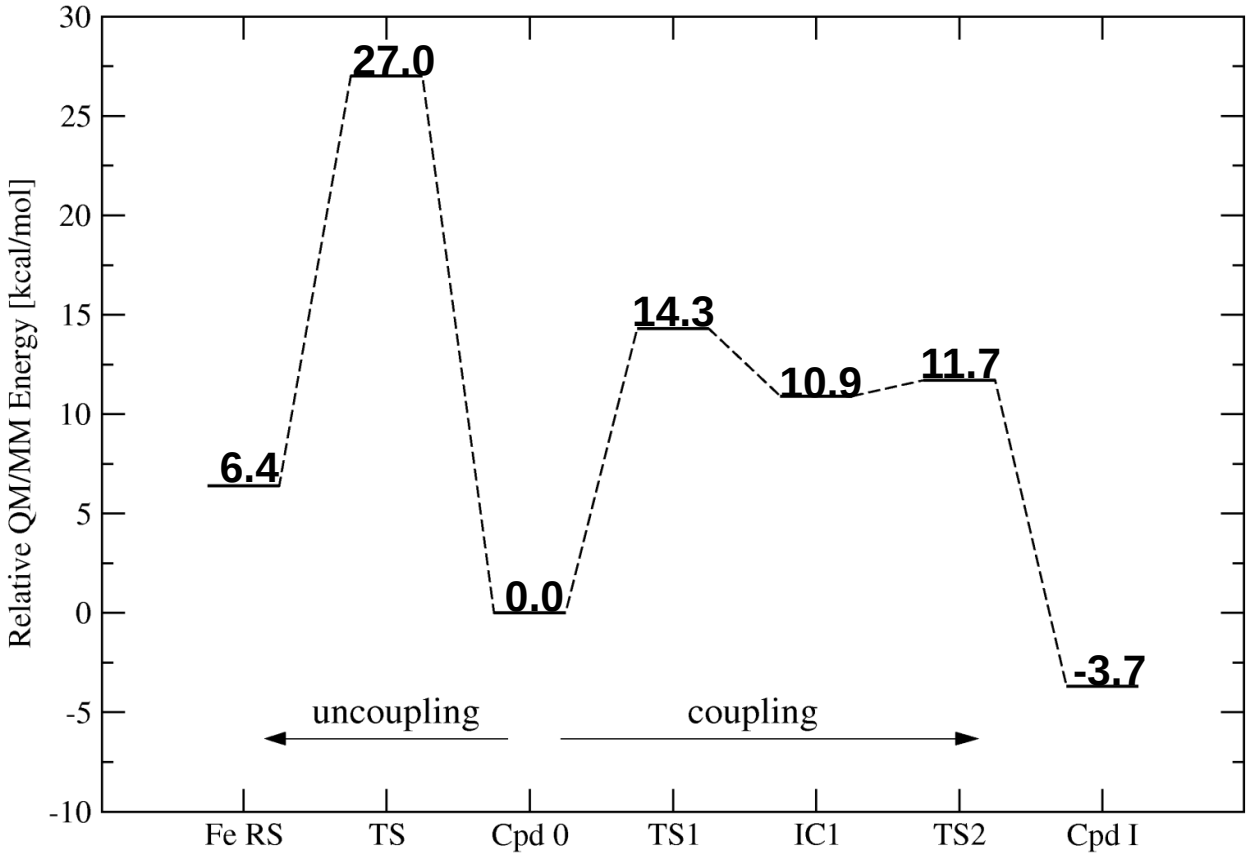

- **The coupling reaction proceeds in two steps. The barrier for initial O-O bond cleavage is around 14 kcal/mol. The second step, proton transfer from Asp251 to OH, is facile (barrier of around 1 kcal/mol).**
- **The uncoupling reaction is concerted (barrier of 27 kcal/mol).**

J. Zheng, D. Wang, W. Thiel, and S. Shaik, J. Am. Chem. Soc. **128**, 13204-13215 (2006).
M. Altarsha, T. Benighaus, D. Kumar, and W. Thiel, J. Am. Chem. Soc. **131**, 4755-4763 (2009).

Coupling and uncoupling reactions T252A and T252A+W mutant

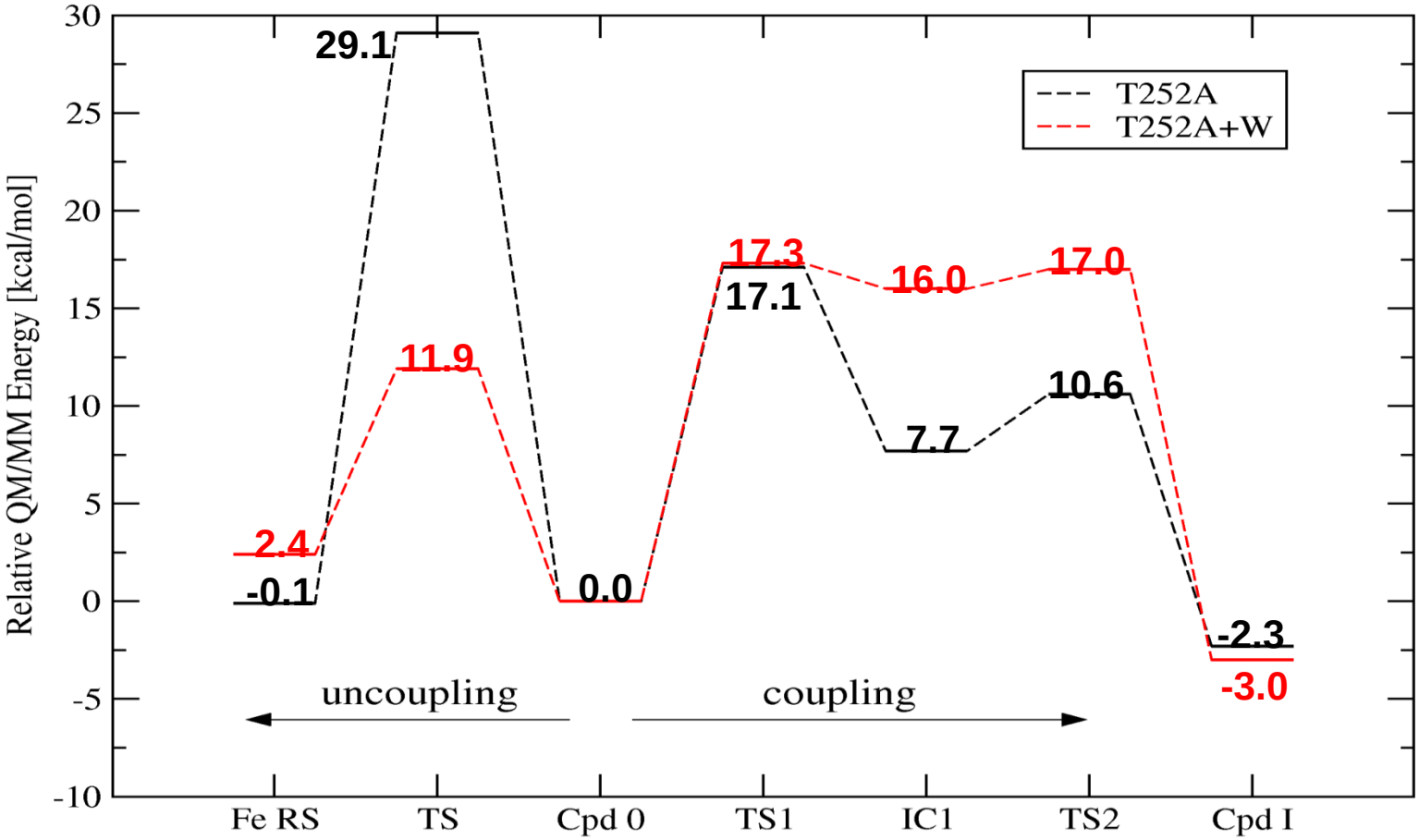

- The barrier for uncoupling is lower than that for coupling.
- WatS does not have much effect on the rate-limiting step of the coupling reaction.
- The presence of an extra water significantly reduces the barrier for the uncoupling reaction.

MD results for T252A: mobility of an extra water molecule

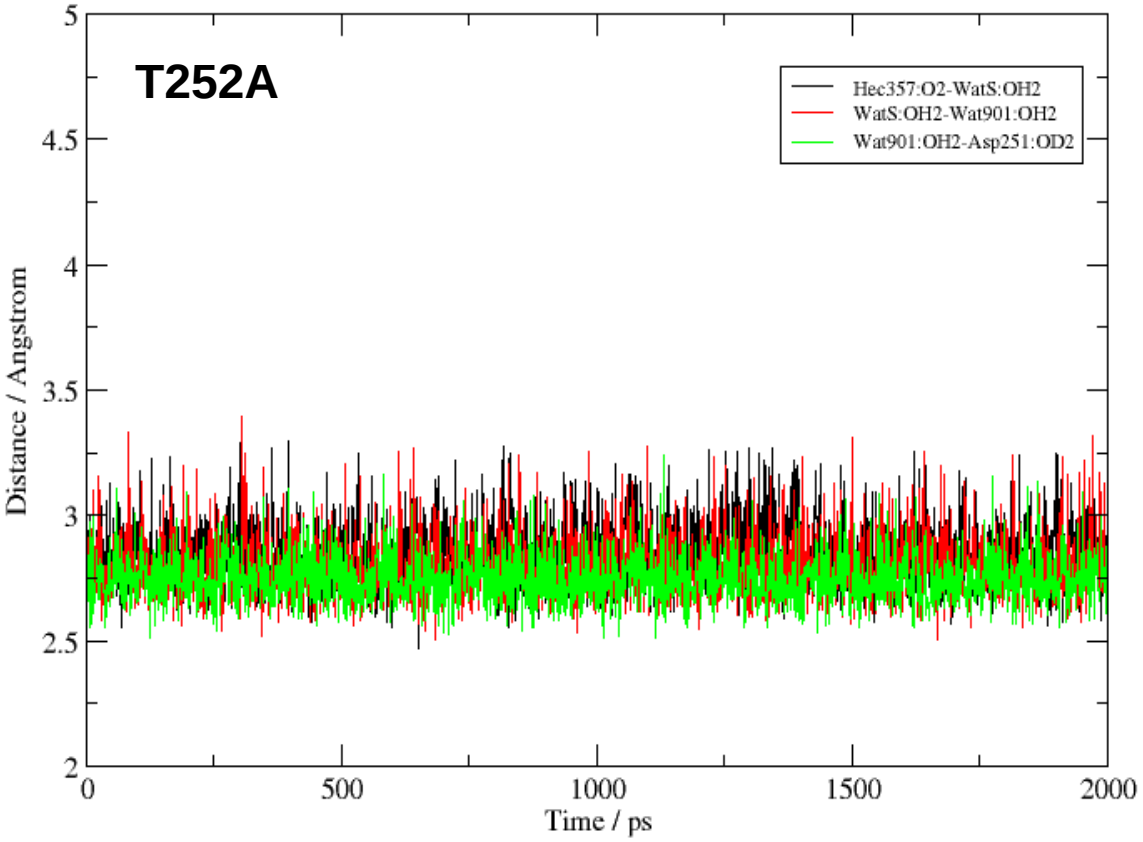

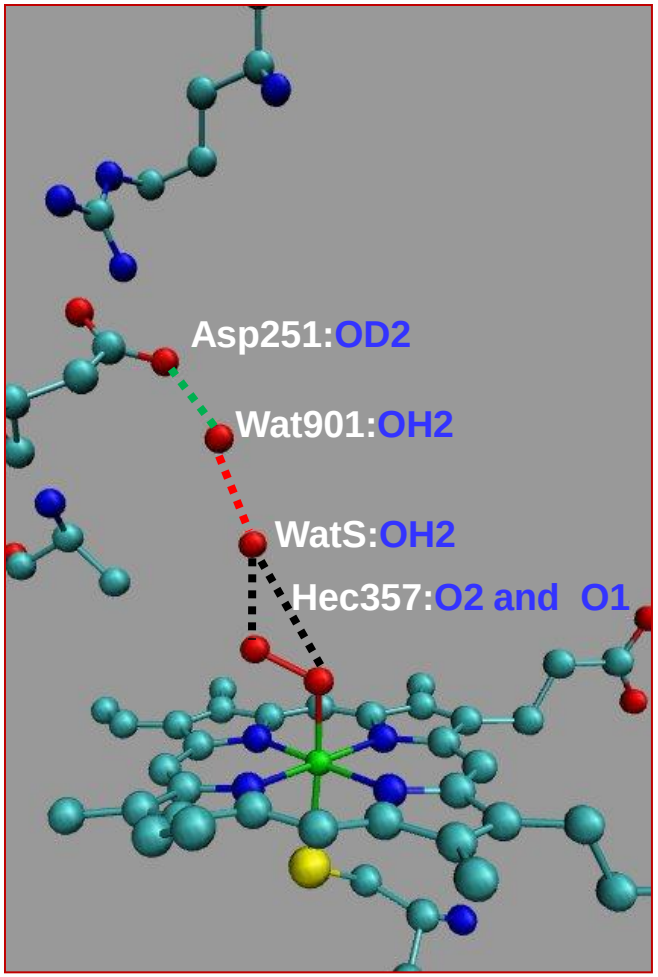

- **Substitution of threonine by alanine generates some empty space in the distal pocket.**
- **Classical MD results for the alanine mutant suggest that Wat901 and WatS do not escape from the protein pocket during 2 ns simulation.**

Rate limiting barriers

Mutant type	Coupling reaction	Uncoupling reaction
WT	14.3	27.0
T252S	15.6	23.1
T252V	17.1	26.5
T252V + W	18.9	19.5
T252A	17.1	29.1
T252A + W	17.3	11.9

- **If the effect of an additional water molecule is not taken into account, all mutants behave like the WT enzyme.**
- **Insertion of an extra water (WatS) has a significant mechanistic effect in the case of the T252V and T252A mutant.**

M. Altarsha, T. Benighaus, D. Kumar, and W. Thiel, J. Am. Chem. Soc. **131**, 4755-4763 (2009).

QM/MM: Status and perspectives

Methodology

- Methods and tools available (not yet black-box approach)
- Including high-level QM components
- Including sampling techniques

Essential for

- Treatment of electronic events in complex systems
- In particular: Chemical reactions
- In particular: Electronic excitation

Useful for

- Unbiased and reliable treatment of complex systems
- Example: Structural refinement
- Example: Ligand binding

Directed evolution tree for *P. aeruginosa* lipase

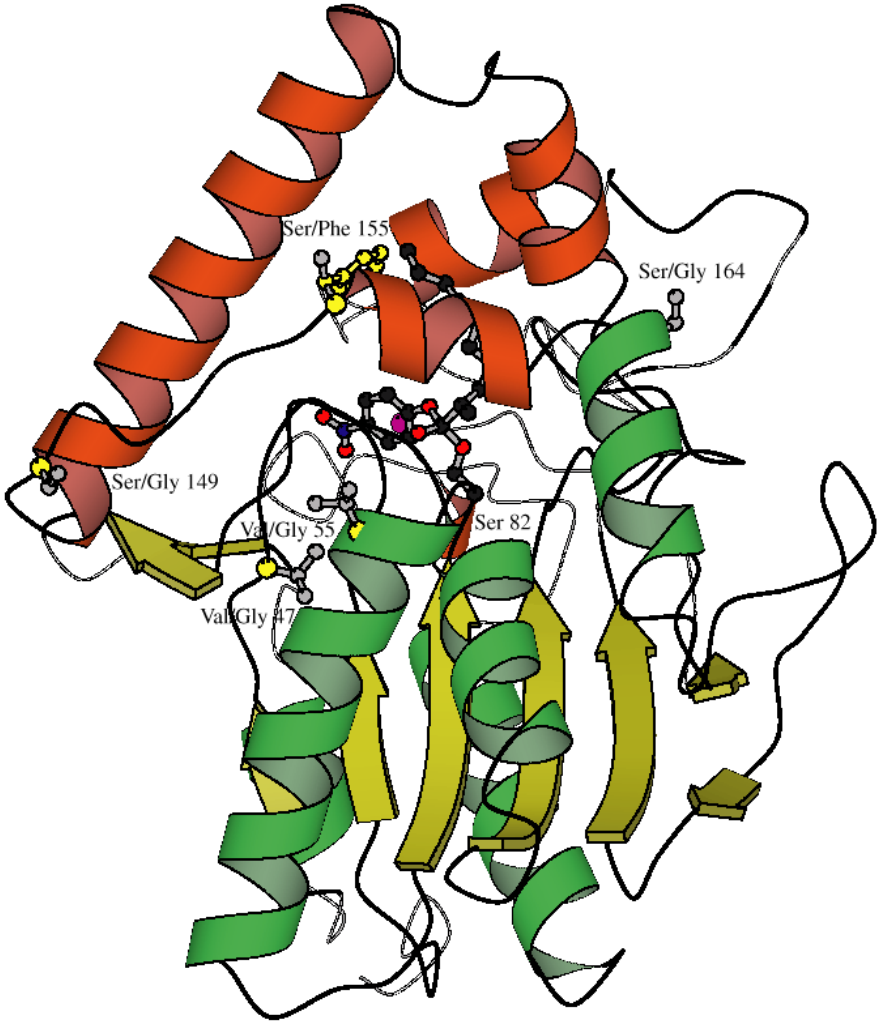

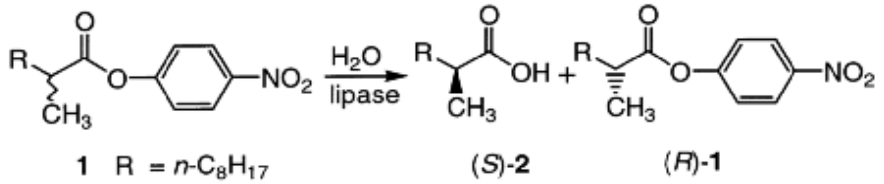

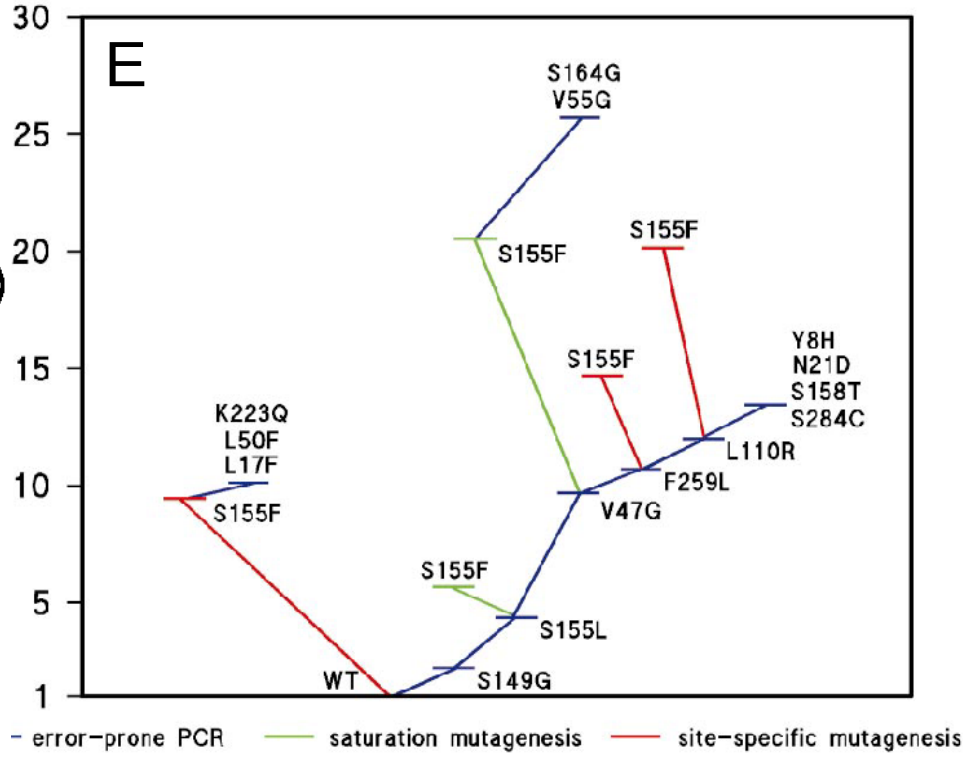

K. Liebeton, A. Zonta, K. Schimossek, M. Nardini, D. Lang, B. W. Dijkstra, M. T. Reetz and K. E. Jaeger, Chem. Biol. **7**, 709 (2000) .

M. T. Reetz, S. Wilensek, D. Zha and K.-E. Jaeger, Angew. Chem. Int. Ed. **40**, 3589 (2001).

P. aeruginosa lipase X-ray structure

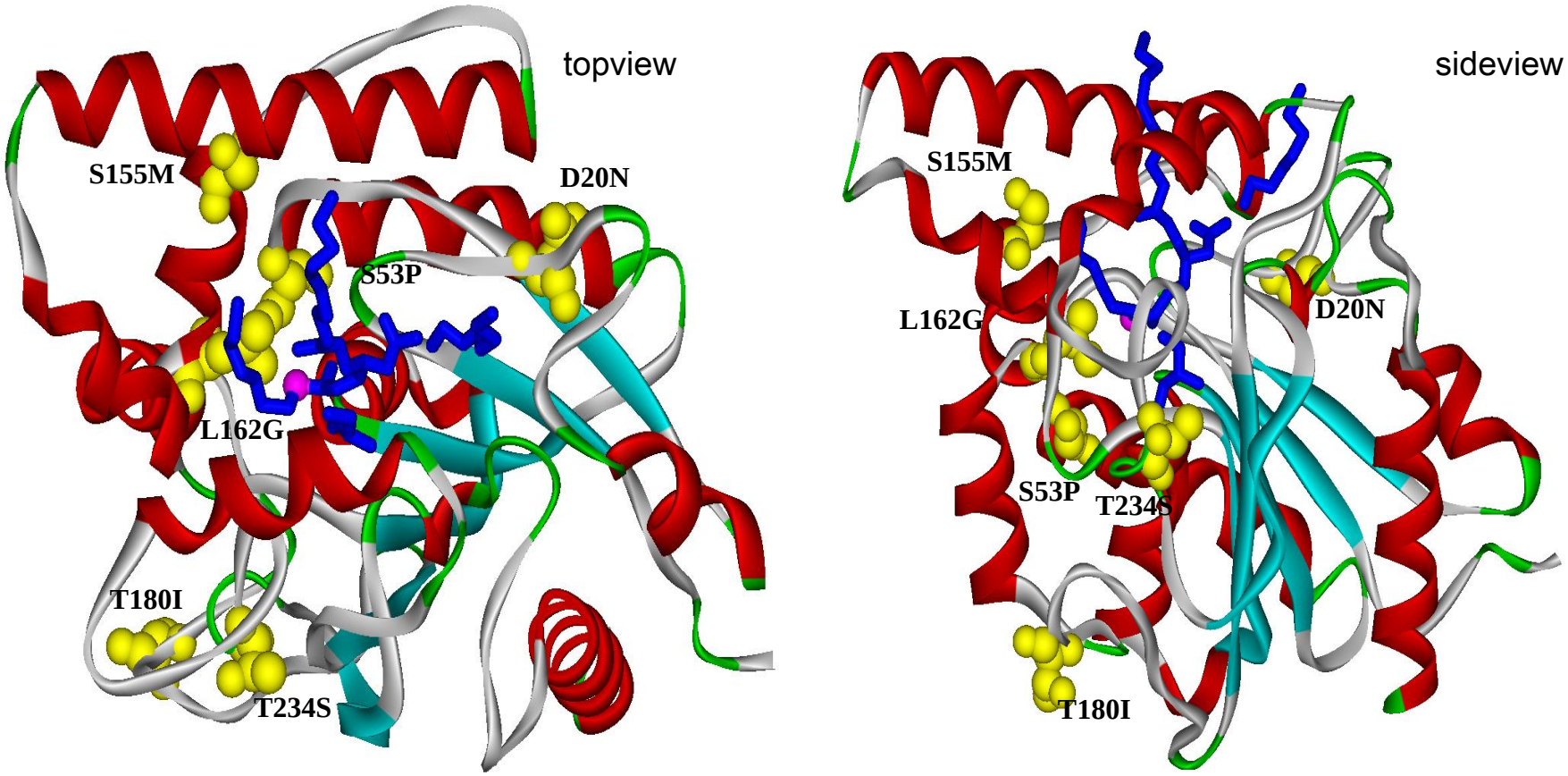

Mutations in yellow, bound phosphonate in blue, C4 phosphonate atom in magenta

X-ray: M. Nardini, D. Lang, K. Liebeton, K. E. Jaeger and B. W. Dijkstra, J. Biol. Chem. **275**, 31219 (2000).
Mutant: M. T. Reetz, S. Wilensek, D. Zha and K. E. Jaeger, Angew. Chem. Int. Ed. **40**, 3589 (2001).

Reaction mechanism in lipases

Lipases cleave ester bonds via a ping-pong mechanism

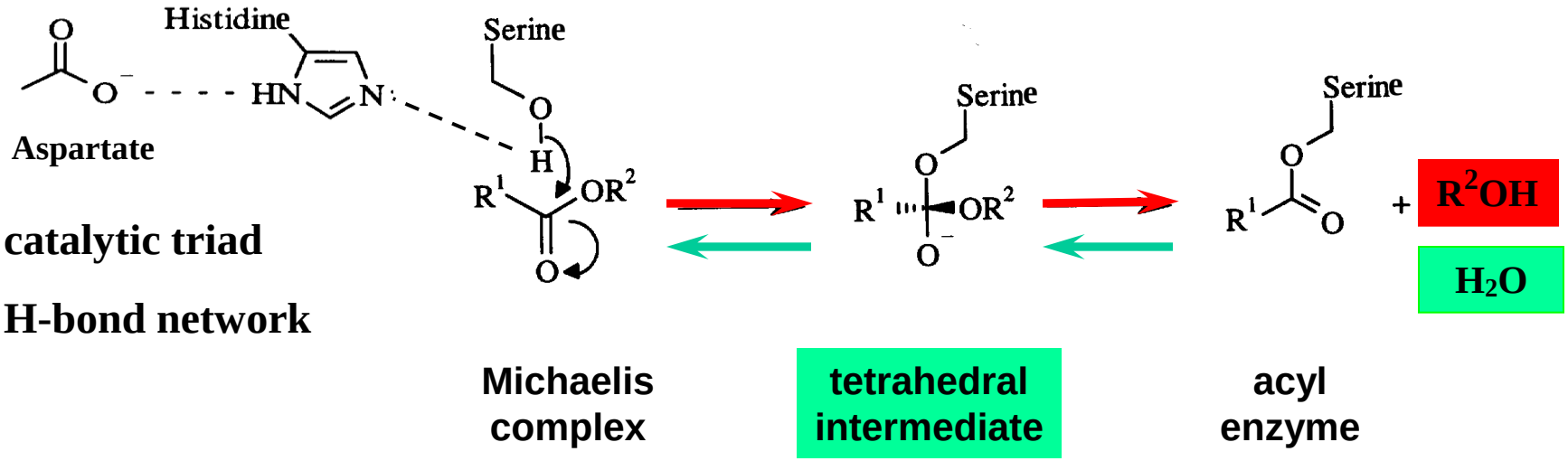

Stabilising the tetrahedral intermediate in a double mutant

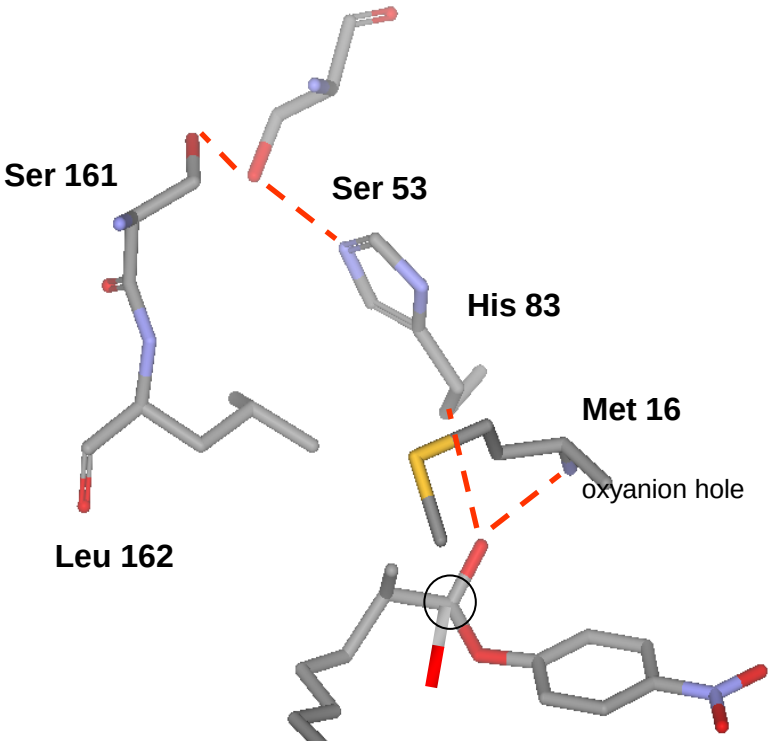

R – MDA ester TI at Ser82

wild-type

X-ray / MD simulation

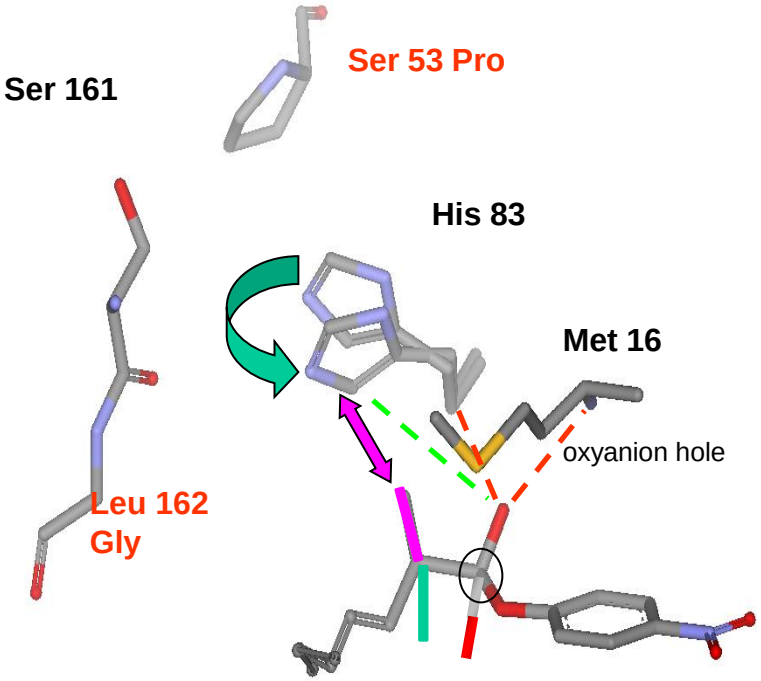

R/S MDA ester TI at Ser82

Ser 53 Pro, Leu 162 Gly

MD simulation

His 83 fixed

His 83 governs stereoselectivity

Follow-up studies on lipase mutants

- **Theoretical prediction (2004)**: Double mutant M8 (S53P/L162G) should enhance S enantioselectivity as well as "best" sixfold mutant X.
- **Experimental verification (2006)**: Targeted synthesis of M8 and measurement of enantioselectivity in the hydrolytic kinetic resolution of racemic substrate.

Enzyme	Conversion (%)	*ee*(%)	E value	
M8	18	96	64	most selective
X	20	95	50	
WT	44	6.8	1.2	

- **Further results** : Substitution of His83 by phenylalanine drastically reduces enantioselectivity (as expected). Replacement of His83 by the small alanine residue retains enantioselectivity because water can enter and provide H-bond stabilization for the S enantiomer.

M. T. Reetz, M. Puls, J. D. Carballeira, A. Vogel, K.-E. Jaeger, T. Eggert, W. Thiel, M. Bocola, and N. Otte, ChemBioChem **8**, 106 (2007).

Acknowledgement

Muhannad Altarsha
Ahmet Altun
Iris Antes
Dirk Bakowies
Tobias Benighaus
Salomon Billeter
Marco Bocola
Johannes Kästner
Devesh Kumar
Hai Lin
Sebastian Metz
Nikolaj Otte
Jan Schöneboom
Hans Martin Senn
Frank Terstegen
Stephan Thiel
Alexander Turner
Tell Tuttle
Mark Waller
Dongqi Wang
Jingjing Zheng

Michael Bühl
Richard Catlow
Bernd Engels
Karl-Erich Jaeger
Christel Marian
Frank Neese
David O'Hagan
Manfred Reetz
Ansgar Schäfer
Sason Shaik
Paul Sherwood
Wilfred van Gunsteren
Hans-Joachim Werner

Support from

Max Planck Society
European Commission (ESPRIT/QUASI)
German-Israeli Foundation for Scientific Research
Volkswagenstiftung
Deutsche Forschungsgemeinschaft (SFB 663)

Our research team in July 2004

Our research team in December 2007